Durant GJ, Ganellin CR, and Parsons ME (1975) Chemical differentiation of histamine H1- and H2-receptor agonists. *J Med Chem* **18:**905–909.
Durie FH, Foy TM, Masters SR, Laman JD, and Noelle RJ (1994) The role of CD40 in the regulation of humoral and cell-mediated immunity. *Immunol Today* **15:** 406–411.
Elenkov IJ, Webster E, Papanicolaou DA, Fleisher TA, Chrousos GP, and Wilder RL (1998) Histamine potently suppresses human IL-12 and stimulates IL-10 production via H2 receptors. *J Immunol* **161:**2586–2593.
Ge J, Jia Q, Liang C, Luo Y, Huang D, Sun A, Wang K, Zou Y, and Chen H (2005) Advanced glycosylation end products might promote atherosclerosis through inducing the immune maturation of dendritic cells. *Arterioscler Thromb Vasc Biol* **25:**2157–2163.
Gill DS, Thompson CS, and Dandona P (1990) Histamine synthesis and catabolism in various tissues in diabetic rats. *Metabolism* **39:**815–818.
Hellstrand K, Asea A, Dahlgren C, and Hermodsson S (1994) Histaminergic regulation of NK cells. Role of monocyte-derived reactive oxygen metabolites. *J Immunol* **153:**4940–4947.
Higuchi S, Tanimoto A, Arima N, Xu H, Murata Y, Hamada T, Makishima K, and Sasaguri Y (2001) Effects of histamine and interleukin-4 synthesized in arterial intima on phagocytosis by monocytes/macrophages in relation to atherosclerosis. *FEBS Lett* **505:**217–22.
Hough LB (2001) Genomics meets histamine receptors: new subtypes, new receptors. *Mol Pharmacol* **59:**415–419.
Johnson CL (1982) Histamine receptors and cyclic nucleotides, in *Pharmacology of Histamine Receptors* (Ganellin CR and Parsons ME, eds) p 146, Wright-PSG, Bristol, UK.
Khan MM, Keaney KM, Melmon KL, Clayberger C, and Krensky AM (1989) Histamine regulates the generation of human cytolytic T lymphocytes. *Cell Immunol* **121:**60–73.
Kohka H, Nishibori M, Iwagaki H, Nakaya N, Yoshino T, Kobashi K, Saeki K, Tanaka N, and Akagi T (2000) Histamine is a potent inducer of IL-18 and IFN-gamma in human peripheral blood mononuclear cells. *J Immunol* **164:**6640–6646.
Li J and Schmidt AM (1997) Characterization and functional analysis of the promoter of RAGE, the receptor for advanced glycation end products. *J Biol Chem* **272:**16498–16506.
Miyazawa N, Watanabe S, Matsuda A, Kondo K, Hashimoto H, Umemura K, and Nakashima M (1998) Role of histamine H1 and H2 receptor antagonists in the prevention of intimal thickening. *Eur J Pharmacol* **362:**53–59.
Morichika T, Takahashi HK, Iwagaki H, Yoshino T, Tamura R, Yokoyama M, Mori S, Akagi T, Nishibori M, and Tanaka N (2003) Histamine inhibits lipopolysaccharide-induced tumor necrosis factor-alpha production in an intercellular adhesion molecule-1- and B7.1-dependent manner. *J Pharmacol Exp Ther* **304:**624–633.
Nakane H, Sonobe Y, Watanabe T, and Nakano K (2004) Histamine: its novel role as an endogenous regulator of Con A-dependent T cell proliferation. *Inflamm Res* **53:**324–328.
Ohtsu H, Kuramasu A, Tanaka S, Terui T, Hirasawa N, Hara M, Makabe-Kobayashi Y, Yamada N, Yanai K, Sakurai E, et al. (2002) Plasma extravasation induced by dietary supplemented histamine in histamine-free mice. *Eur J Immunol* **32:**1698–1708.
Okamoto T, Yamagishi S, Inagaki Y, Amano S, Koga K, Abe R, Takeuchi M, Ohno S, Yoshimura A, and Makita Z (2002) Angiogenesis induced by advanced glycation end products and its prevention by cerivastatin. *FASEB J* **16:**1928–1930.
Parsons ME, Owen DA, Ganellin CR, and Durant GJ (1977) Dimaprit—(*S*-[3-(*N,N*-dimethylamino)prophyl]isothiourea)—a highly specific histamine H2-receptor agonist. Part 1. Pharmacology. *Agents Actions* **7:**31–37.
Ranger AM, Das MP, Kuchroo VK, and Glimcher LH (1996) B7-2 (CD86) is essential for the development of IL-4-producing T cells. *Int Immunol* **8:**1549–1560.
Ruderman NB, Williamson JR, and Brownlee M (1992) Glucose and diabetic vascular disease. *FASEB J* **6:**2905–2914.
Sasaguri Y, Wang KY, Tanimoto A, Tsutsui M, Ueno H, Murata Y, Kohno Y, Yamada S, and Ohtsu H (2005) Role of histamine produced by bone marrow-derived vascular cells in pathogenesis of atherosclerosis. *Circ Res* **96:**974–981.
Schmidt AM, Hasu M, Popov D, Zhang JH, Chen J, Yan SD, Brett J, Cao R, Kuwabara K, Costache G, Simonescut N, Simonescut M, and Stern D (1994) Receptor for advanced glycation end products (AGEs) has a central role in vessel wall interactions and gene activation in response to circulating AGE proteins. *Proc Natl Acad Sci USA* **91:**8807–8811.
Shayo C, Davio C, Brodsky A, Mladovan AG, Legnazzi BL, Rivera E, and Baldi A (1997) Histamine modulates the expression of c-fos through cyclic AMP production via the H2 receptor in the human promonocytic cell line U937. *Mol Pharmacol* **51:**983–990.
Stoll G and Bendszus M (2006) Inflammation and atherosclerosis: novel insights into plaque formation and destabilization. *Stroke* **37:**1923–1932.
Takahashi HK, Iwagaki H, Tamura R, Xue D, Sano M, Mori S, Yoshino T, Tanaka N, and Nishibori M (2003) Unique regulation profile of prostaglandin E1 on adhesion molecule expression and cytokine production in human peripheral blood mononuclear cells. *J Pharmacol Exp Ther* **307:**1188–1195.
Takahashi HK, Mori S, Wake H, Liu K, Yoshino T, Ohashi K, Tanaka N, Shikata K, Makino H, and Nishibori M (2009) Advanced glycation end products subspecies-selectively induce adhesion molecule expression and cytokine production in human peripheral blood mononuclear cells. *J Pharmacol Exp Ther* **330:**89–98.
Takahashi HK, Watanabe T, Yokoyama A, Iwagaki H, Yoshino T, Tanaka N, and Nishibori M (2006) Cimetidine induces interleukin-18 production through H2-agonist activity in monocytes. *Mol Pharmacol* **70:**450–453.
Takahashi HK, Yoshida A, Iwagaki H, Yoshino T, Itoh H, Morichika T, Yokoyama M, Akagi T, Tanaka N, Mori S, et al. (2002) Histamine regulation of interleukin-18-initiating cytokine cascade is associated with down-regulation of intercellular adhesion molecule-1 expression in human peripheral blood mononuclear cells. *J Pharmacol Exp Ther* **300:**227–235.
Takedo A, Yasuda T, Miyata T, Mizuno K, Li M, Yoneyama S, Horie K, Maeda K, and Sobue G (1996) Immunohistochemical study of advanced glycation end products in aging and Alzheimer's disease brain. *Neurosci Lett* **221:**17–20.
Takeuchi M and Yamagishi S (2004) TAGE (toxic AGEs) hypothesis in various chronic diseases. *Med Hypotheses* **63:**449–452.
Takeuchi M, Makita Z, Bucala R, Suzuki T, Koike T, and Kameda Y (2000) Immunological evidence that non-carboxymethyllysine advanced glycation end-products are produced from short chain sugars and dicarbonyl compounds in vivo. *Mol Med* **6:**114–125.
Tanimoto A, Sasaguri Y, and Ohtsu H (2006) Histamine network in atherosclerosis. *Trends Cardiovasc Med* **16:**280–284.
Tanimoto A, Wang KY, Murata Y, Kimura S, Nomaguchi M, Nakata S, Tsutsui M, and Sasaguri Y (2007) Histamine upregulates the expression of inducible nitric oxide synthase in human intimal smooth muscle cells via histamine H1 receptor and NF-kappaB signaling pathway. *Arterioscler Thromb Vasc Biol* **27:**1556–1561.
van der Pouw Kraan TC, Snijders A, Boeije LC, de Groot ER, Alewijnse AE, Leurs R, and Aarden LA (1998) Histamine inhibits the production of interleukin-12 through interaction with H2 receptors. *J Clin Invest* **102:**1866–1873.
Vlassara H and Palace MR (2002) Diabetes and advanced glycation endproducts. *J Intern Med* **251:**87–101.
Yamagishi S and Imaizumi T (2005) Diabetic vascular complications: pathophysiology, biochemical basis and potential therapeutic strategy. *Curr Pharm Des* **11:** 2279–2299.

Address correspondence to: Dr. Masahiro Nishibori, Department of Pharmacology, Okayama University Graduate School of Medicine and Dentistry, 2-5-1 Shikata-cho, Okayama 700-8558, Japan. E-mail: mbori@md.okayama-u.ac.jp

Acta Med. Okayama, 2009
Vol. 63, No. 4, pp. 203-211

Acta Medica Okayama
http://escholarship.lib.okayama-u.ac.jp/amo/

Original Article

Establishment of *in Vitro* Binding Assay of High Mobility Group Box-1 and S100A12 to Receptor for Advanced Glycation Endproducts: Heparin's Effect on Binding

Rui Liu[a,b], Shuji Mori[c], Hidenori Wake[b], Jiyong Zhang[b], Keyue Liu[b], Yasuhisa Izushi[b], Hideo K. Takahashi[b], Bo Peng[a], and Masahiro Nishibori[b]*

[a]*Shanghai University of Traditional Chinese Medicine, Shanghai 201-203, China,* [b]*Department of Pharmacology, Okayama University Graduate School of Medicine, Dentistry and Pharmaceutical Sciences, Okayama 700-8558, Japan, and* [c]*Shujitsu University, School of Pharmacy, Okayama 703-8516, Japan*

Interaction between the receptor for advanced glycation end products (RAGE) and its ligands has been implicated in the pathogenesis of various inflammatory disorders. In this study, we establish an *in vitro* binding assay in which recombinant human high-mobility group box 1 (rhHMGB1) or recombinant human S100A12 (rhS100A12) immobilized on the microplate binds to recombinant soluble RAGE (rsRAGE). The rsRAGE binding to both rhHMGB1 and rhS100A12 was saturable and dependent on the immobilized ligands. The binding of rsRAGE to rhS100A12 depended on Ca^{2+} and Zn^{2+}, whereas that to rhHMGB1 was not. Scatchard plot analysis showed that rsRAGE had higher affinity for rhHMGB1 than for rhS100A12. rsRAGE was demonstrated to bind to heparin, and rhS100A12, in the presence of Ca^{2+}, was also found to bind to heparin. We examined the effects of heparin preparations with different molecular sizes—unfractionated native heparin (UFH), low molecular weight heparin (LMWH) 5000 Da, and LMWH 3000 Da— on the binding of rsRAGE to rhHMGB1 and rhS100A12. All 3 preparations concentration-dependently inhibited the binding of rsRAGE to rhHMGB1 to a greater extent than did rhS100A12. These results suggested that heparin's anti-inflammatory effects can be partly explained by its blocking of the interaction between HMGB1 or S100A12 and RAGE. On the other hand, heparin would be a promising effective remedy against RAGE-related inflammatory disorders.

Key words: RAGE, HMGB1, S100A12, heparin, inflammation

The receptor for advanced glycation end products (RAGE) is a member of the immunoglobulin superfamily of cell-surface molecules, which has been suggested to be involved in sustaining and amplifying inflammatory responses [1, 2]. RAGE can recognize a wide range of endogenous ligands, such as advanced glycation end products (AGEs), amyloid-β peptide (Aβ), high mobility group box 1 (HMGB1), and the S100/calgranulin family [3]. RAGE's structure includes an extracellular immunoglobulin-like region essential for its binding to ligands, a single transmembrane domain, and a short cytoplasmic tail responsible for RAGE-mediated signal transduction [4]. There are soluble forms of RAGE—endogenous secretory RAGE (esRAGE) and soluble RAGE (sRAGE)—that lack a transmembrane domain and act

Received April 22, 2009; accepted June 23, 2009.
*Corresponding author. Phone:+81-86-235-7140; Fax:+81-86-235-7140
E-mail:mbori@md.okayama-u.ac.jp (M. Nishibori)

as decoy receptors [5]. The binding of ligands to RAGE triggers intracellular signaling such as nuclear factor kappa B (NF-κB) and mitogen-activated protein kinase (MAPK) activation in vascular endothelial cells and macrophages, leading to the development of inflammation-based diseases, such as diabetic complications, sepsis, Alzheimer's and rheumatic arthritis [6–9]. As a result, interfering with the binding of ligands to RAGE has been thought to be a means with which to block the inflammatory responses sustained by RAGE-dependent pathways.

Among the RAGE ligands, AGEs are the groups of nonenzymatically glycosylated proteins that accumulate in vascular tissue in a wide variety of disorders, especially in diabetes [10]. HMGB1 is a ubiquitous and abundant nuclear protein, which can be passively released from necrotic cells and actively secreted by macrophages. After HMGB1 is released into the extracellular environment, it functions as a pro-inflammatory mediator [11, 12]. S100/calgranulin is a multigenic family of EF-hand Ca^{2+}-binding proteins [13]. S100A12 is one member of the S100 protein family, which is found mainly in neutrophil granulocytes and monocytes [14]. S100A12 has a role in cell homeostasis as an intracellular molecule, but contributes to the pathogenesis of inflammatory lesions via interaction with RAGE after release to the extracellular compartment [15].

Heparin is a highly sulfated glycosaminoglycan, which has been traditionally used clinically as an anticoagulant [16]. It is biosynthesized and stored in the granules of mast cells [17]. More recent studies have highlighted the role of heparin as an anti-inflammatory substance that has been used in the treatment of some inflammatory settings [18–20]. However, the molecular mechanisms underlying the anti-inflammation activities of heparin remain to be determined. Antagonism of AGE's effect by LMWH *in vivo* has been reported [21]. A similar effect of heparin on AGE-RAGE signaling also has been demonstrated by the inhibition of RAGE-dependent NF-κB activation in glioma cells and expression of vascular cell adhesion molecule-1 (VCAM-1) and vascular endothelial growth factor (VEGF) in endothelial cells. HMGB1 has also been described as a heparin-binding protein [22–24]. Therefore, heparin may be an important regulator of RAGE-mediated responses through multiple ligands.

To investigate the complex binding properties of RAGE to many ligands, we attempted to establish *in vitro* binding of sRAGE to HMGB1 and S100A12 using a microplate. Both *in vitro* binding assays were saturated in terms of sRAGE and ligands. We clearly showed Ca^{2+}, Zn^{2+}-dependent binding of S100A12 to sRAGE. We also observed the binding inhibition activity of each of the 3 heparin preparations, suggesting a mechanism for heparin's anti-inflammatory activity. This may provide insights into potential uses of heparin in some RAGE-related pathologies.

Materials and Methods

Materials. Recombinant plasmid pASK-IBA32-sRAGE was transformed into *E.coli* BL 21 (DE3) (Merck, San Diego, LA), and recombinant sRAGE (rsRAGE) proteins with a 6-histidine tag were expressed. rsRAGE proteins were partially purified by using a Ni-NTA column and further purified by heparin-sepharose affinity chromatography. Recombinant plasmids pGEX-6P-1-HMGB1 and pGEX-6P-1-S100A12 were transformed into *E.coli* BL 21 (DE3). Recombinant human HMGB1 (rhHMGB1) and recombinant human S100A12 (rhS100A12) proteins were expressed as GST-HMGB1 or GST-S100A12 fusion proteins, respectively. GST tag was cleaved by protease in Glutathione Sepharose™ 4B columns. Unfractionated heparin (UFH) (mol wt: 12000～15000 Da), low molecular weight heparin (LMWH) (mol wt: 5000 Da or 3000 Da), and bovine serum albumin (BSA) were purchased from Sigma-Aldrich (St. Louis, MO, USA). 2, 2'-Azino-bis (3-ethylbenzthiazoline-6-sulphonic acid) (ABTS) was a product of Tokyo Kasei. Kogyo. (Tokyo, Japan). Ni-NTA HRP Conjugate was from QIAGEN (Hilden, Germany). A 96-well ELISA plate (SUMILON®, MS-8696F) was purchased from Sumitomo Bakelite (Tokyo, Japan).

Binding assay of rsRAGE to rhHMGB1 or rhS100A12. A flat-bottom 96-well plate was coated overnight with various concentrations of rhHMGB1 or rhS100A12 at 4°C (50μl/well). Control wells received only PBS (50μl/well). The plates were washed with PBS (200μl/well) 3 times and blocked with 10% (w/v) BSA in PBS (100μl/well) for 2h at room temperature. After unbound rhHMGB1 or rhS100A12 was washed off, different concentrations of rsRAGE diluted with 10% BSA in PBS were

added into wells in triplicate (50 μl/well), and incubation continued overnight at 4°C. Unbound rsRAGE was removed by washing 3 times with PBS at room temperature. Ni-NTA HRP Conjugate 1/500 diluted by 0.2% BSA in PBS (100 μl/well) was added to the wells and incubated for 2 h at 4°C. After washing with PBS, substrate solution, 0.1% ABTS dissolved in 20 mM phosphate-citrate buffer (pH 5.0) was added to each well (50 μl/well) and incubated for 30 min at room temperature. Finally, a stop solution of 1% SDS was added (100 μl/well). The absorbance was measured at 415 nm in a microplate reader (Model 680) from Bio-Rad Laboratories (Hercules, CA, USA).

To determine the effects of divalent cations on the binding, experiments for rsRAGE binding to rhHMGB1 were performed with PBS buffer containing no divalent cations; 1 mM $CaCl_2$; 1 mM $CaCl_2$ and 10 μM $ZnCl_2$ throughout, and the experiments for rsRAGE binding to rhS100A12 were performed with PBS buffer containing no divalent cations; 1 mM $CaCl_2$; 1 mM $CaCl_2$ and 0.5 mM $MgCl_2$; 1 mM $CaCl_2$ and 10 μM $ZnCl_2$; 1 mM $CaCl_2$ and 0.5 mM $MgCl_2$ and 10 μM $ZnCl_2$ throughout. rsRAGE and rhHMGB1 were incubated for 24 h, 48 h, and 72 h at 4°C, respectively, to determine the effect of incubation time on the binding of rsRAGE to rhHMGB1.

rsRAGE was purified by heparin-sepharose affinity chromatography. rsRAGE, partially purified by using a Ni-NTA column, was further purified by heparin-sepharose affinity chromatography. Heparin-sepharose CL-6B (GE Healthcare, Milwaukee, WI, USA) was poured into the column and equilibrated with 20 mM phosphate buffer (pH 7.4) containing 150 mM NaCl. rsRAGE was mixed with heparin-sepharose for 3 h at 4°C. The supernatant was removed after centrifugation for 15 min at 1,500 rpm. rsRAGE was eluted with buffer containing 600 mM NaCl after washing with buffer containing 150 mM NaCl. Purified rsRAGE was analyzed by SDS-PAGE.

Binding of rhS100A12 to heparin-sepharose. 100 μl of 50% heparin-sepharose slurry was washed with 200 μl PBS by centrifugation at 1,500 rpm for 5 min twice. PBS containing 1 mM EDTA, no divalent cations, or 1 mM Ca^{2+} was used throughout the experiment. To the washed gel was added 200 μl of rhS100A12. Samples were mixed in rotation at 4°C for 3 h. The supernatant and the sepharose gel were incubated with SDS-PAGE sample buffer at 99°C for 5 min in a shaker. Then, 15 μl of each sample was electrophoresed by SDS-PAGE.

The effects of different preparations of heparin with diverse molecular weights on the binding of rsRAGE to rhHMGB1 or rhS100A12. rhHMGB1 or rhS100A12 was coated on the plate as described above. Then, 25 μg/ml rsRAGE was incubated with various concentration of heparin preparations diluted by 10% BSA in PBS for 30 min at 4°C, and the mixture was added to the plate (50 μl/well). The following procedures were the same as those described above in the binding assay.

Results

rsRAGE binding to rhHMGB1. Different concentrations of rhHMGB1 were immobilized on 96-well plates, and then various concentrations of rsRAGE were added to the plate. Bound sRAGE was determined by the addition of Ni-NTA HRP followed by the peroxidase reaction. The total binding was dependent on both rhHMGB1 and rsRAGE (Fig. 1A). The binding was saturable with respect to the rsRAGE concentration (Fig. 1B). The values of nonspecific binding in the absence of rhHMGB1 were very small compared with the specific binding. The inset shows a Scatchard plot of the specific binding obtained with rhHMGB1 at 6 μg/ml for coating. The K_d value of sRAGE for rhHMGB1 determined from the Scatchard analysis was 0.71 μM. rsRAGE bound to rhHMGB1 also in a time-dependent manner (Fig. 2). The presence of Ca^{2+} (1 mM) on the combination did not influence the binding of rsRAGE to rhHMGB1 (Fig. 3).

rsRAGE binding to rhS100A12. Since S100A12 has been demonstrated to be a Ca^{2+}- and Zn^{2+}-binding EF-hand protein [28], we examined the effects of divalent cations on rsRAGE binding to rhS100A12. Ca^{2+} (1 mM) alone significantly increased the binding of rsRAGE to rhS100A12, by 3-fold. Zn^{2+} (10 μM) further enhanced binding, while Mg^{2+} (0.5 mM) had no effect on it (Fig. 4). These results implied that Ca^{2+}- and Zn^{2+}-bound conformation of S100A12 is required for the optimal binding to rsRAGE. Fig. 5A shows the total and specific binding of rsRAGE to immobilized rhS100A12 (2 μg/ml, 10 μg/ml, and 50 μg/ml for the coating plate) in the

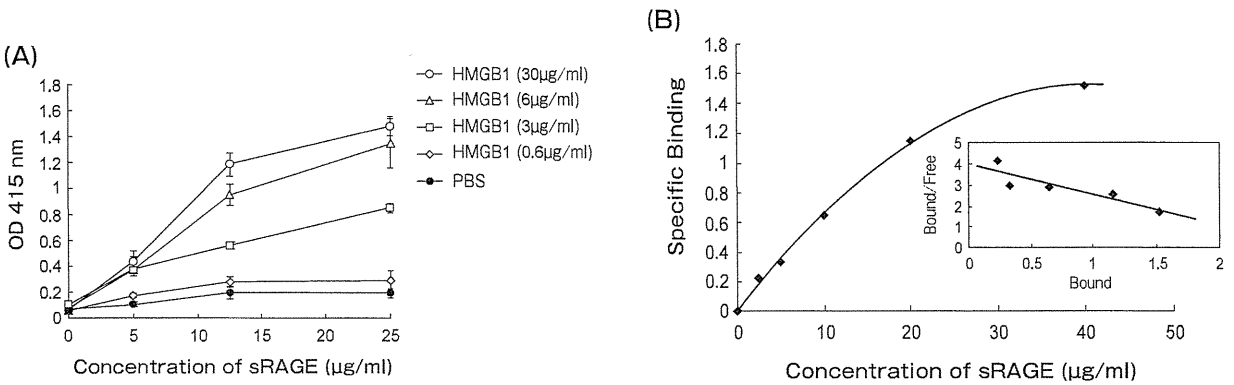

Fig. 1 Concentration-dependent binding of rsRAGE to rhHMGB1. (A) Different concentrations of rhHMGB1 were immobilized onto the wells of a 96-well plate. After blocking the plate with 10% BSA/PBS, the indicated concentrations of rsRAGE were added to the wells. The bound rsRAGE was quantified as described in Methods. The results were the means ± SEM of 3 independent experiments. (B) Specific binding of rsRAGE to rhHMGB1 was calculated by subtracting nonspecific binding in the absence of rhHMGB1 from the total binding with 6μg/ml of rhHMGB1. The inset shows the Scatchard plot of the saturation curve. The K_d value of rsRAGE for rhHMGB1 binding was estimated to be 0.71μM.

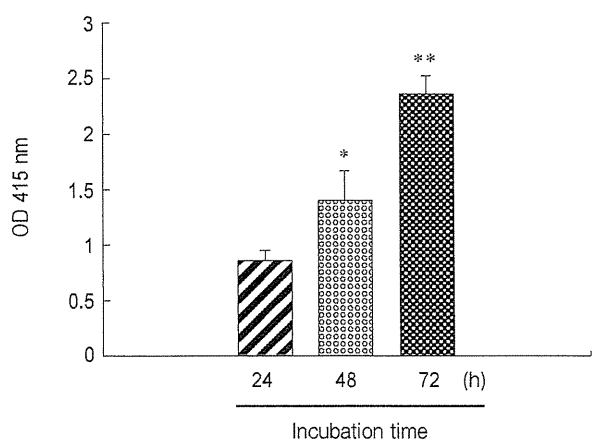

Fig. 2 Time-dependent binding of rsRAGE to rhHMGB1. First, 3μg/ml of rhHMGB1 was immobilized onto each well of a 96-well plate. After the plate was blocked with 10% BSA/PBS, 25μg/ml of rsRAGE was added to each well and the incubation continued for 24h, 48h, and 72h at 4°C. The results were the means ± SEM of 3 independent experiments. $^*P<0.05$, $^{**}P<0.01$ compared with the value at 24h.

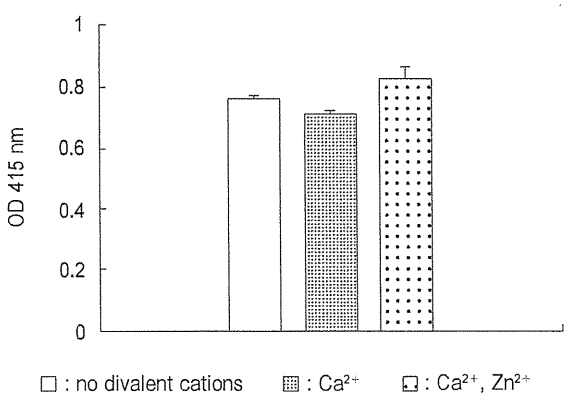

Fig. 3 The effects of Ca^{2+} and Zn^{2+} on rsRAGE binding to rhHMGB1. The plate was coated with 6μg/ml rhHMGB1, and 12.5μg/ml rsRAGE was added to each well. 1mM Ca^{2+} and 10μM Zn^{2+} were added to the well indicated at the start of plate coating and were present throughout the period immediately before the final reaction. The results were the means ± SEM of 3 independent experiments.

presence of Ca^{2+} and Zn^{2+}. The K_d value of rsRAGE for rhS100A12 binding was determined to be 1.39μM by Scatchard analysis, as shown in the inset (Fig. 5B).

rsRAGE was purified by heparin-sepharose affinity chromatography. The fractions obtained from heparin-sepharose affinity chromatography were run on SDS-PAGE gels under denaturing conditions. Coomassie brilliant blue staining showed the presence of rsRAGE with a molecular size of 45000 Da (Fig. 6), which strongly suggested that rsRAGE can be regarded as a heparin-binding protein.

rhS100A12 binding to heparin-sepharose. After rhS100A12 was incubated with heparin-sepharose, the supernatant and the sepharose gel were analyzed by SDS-PAGE under denaturing conditions and

Coomassie brilliant blue staining. rhS100A12 bound to heparin-sepharose also in a Ca^{2+}-dependent manner. A band was obtained with a molecular size of 11000 Da in the presence of Ca^{2+}, while there was no clear band in the presence of EDTA or in the absence of Ca^{2+} (Fig. 7).

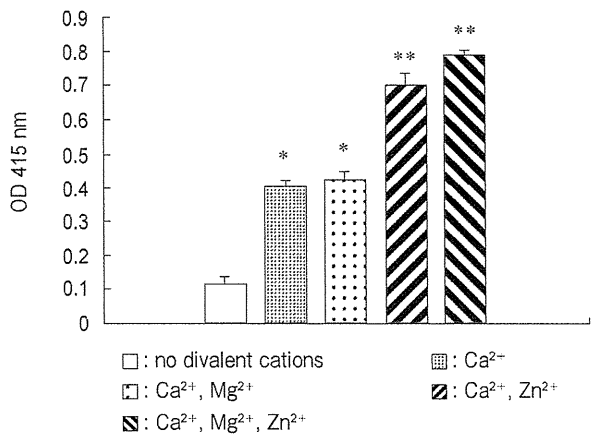

Fig. 4 The effects of divalent cations on rsRAGE binding to rhS100A12. The plate was coated with 50 μg/ml rhS100A12, and 25 μg/ml rsRAGE was added to each well. Ca^{2+}, Zn^{2+}, and Mg^{2+} were added to the wells indicated at the start of plate coating and were present throughout the period immediately before the final reaction. The results were the means ± SEM of 3 independent experiments. $^{*}P<0.05$, $^{**}P<0.01$ compared with the value with no divalent cations.

Heparin inhibits the binding of rsRAGE to rhHMGB1. The effects of each of the 3 preparations of heparin with different average molecular weights on rsRAGE binding to rhHMGB1 were examined. The concentrations of rhHMGB1 and rsRAGE were fixed at 3 μg/ml and 25 μg/ml, respectively. All 3 preparations concentration-dependently inhibited the binding of rsRAGE to rhHMGB1 from 0.5 to 2 μg/ml (Fig. 8). The rank order of inhibitory potency was UFH, LMWH 5000 Da, and LMWH 3000 Da.

Heparin inhibits the binding of rsRAGE to rhS100A12. The effects of the 3 preparations of heparin with different average molecular weights on the binding of rsRAGE to rhS100A12 were evaluated in the presence of 1mM Ca^{2+} and 10 μM Zn^{2+}. The concentrations of S100A12 and rsRAGE were fixed at 50 μg/ml and 25 μg/ml, respectively. Similar to the effects on the binding of rhHMGB1 to rsRAGE, all 3 preparations concentration-dependently inhibited the binding of rsRAGE to rhS100A12 (Fig. 9). However, the inhibitory potency against S100A12 binding was much lower than that against HMGB1 binding, and that was common to all 3 preparations. Even at 100 μg/ml of heparin, the inhibition was about 50%, irrespective of the preparation.

Discussion

RAGE is a transmembrane protein and has been

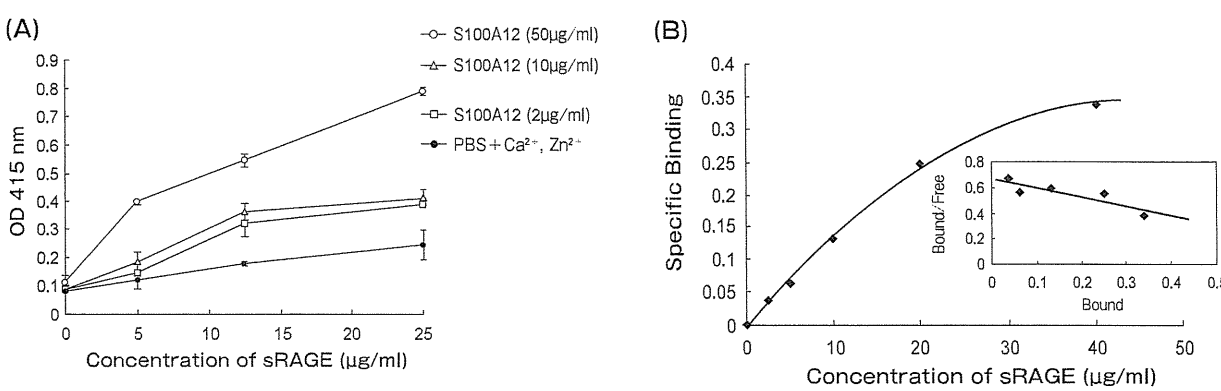

Fig. 5 Concentration-dependent binding of rsRAGE to rhS100A12. (A) Different concentrations of rhS100A12 were immobilized onto the wells of a 96-well plate in the presence of 1mM Ca^{2+}, 10 μM Zn^{2+}, and 0.5mM Mg^{2+}. After the plate was blocked with 10% BSA/PBS, the indicated concentrations of rsRAGE were added to the wells. Ca^{2+}, Zn^{2+}, and Mg^{2+} were present throughout the period immediately before the final reaction. The results were the means ± SEM of 3 independent experiments. (B) Specific binding of rsRAGE to rhS100A12 was calculated by subtracting nonspecific binding in the absence of rhHMGB1 from the total binding with 50 μg/ml rhS100A12. The inset shows the Scatchard plot of the saturation curve. The K_d value of rsRAGE for rhS100A12 binding was estimated to be 1.39 μM.

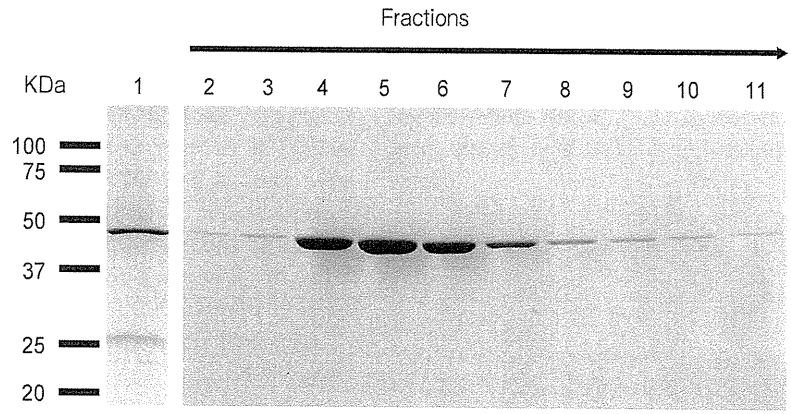

Fig. 6 Purification of rsRAGE using heparin-sepharose affinity chromatography. Partially purified rsRAGE preparations by using a Ni-NTA column (lane 1) were applied to heparin-sepharose. The bound proteins were eluted with 600 mM NaCl (lanes 4-11) after extensive washing (lanes 2 and 3). The eluted samples were electrophoresed on 12% separation gel, and SDS-PAGE gel was stained with Coomassie brilliant blue.

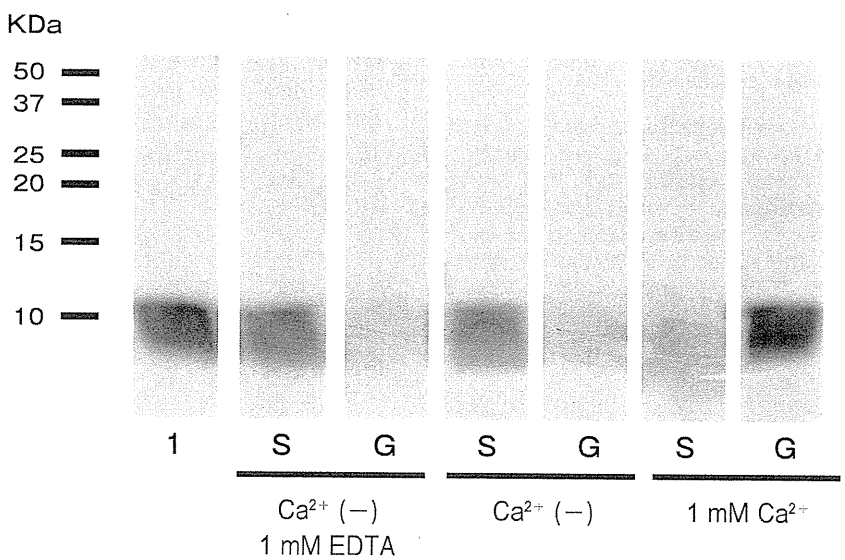

Fig. 7 rhS100A12 binding to heparin-sepharose. rhS100A12 was mixed with heparin-sepharose for 3h at 4°C under different Ca^{2+} condition. After incubation, the supernatant (S) and the sepharose gel (G) were electrophoresed on 15% separation gel, and the SDS-PAGE gel was stained with Coomassie brilliant blue. Lane 1, loading S100A12.

reported to be a receptor for several ligands including HMGB1, S100A12, S100A8/9, AGEs, and Aβ. RAGE belongs to the immunoglobulin superfamily and has 3 immunoglobulin-like domain structures in the extracellular portion. We used recombinant human soluble RAGE with a 6-histidine tag at the C-terminus for the *in vitro* binding and established the binding assay of HMGB1 or S100A12 to RAGE.

The binding of rhHMGB1 to rsRAGE was concentration-dependent and time-dependent (Fig. 1 and Fig. 2). The binding was saturable in terms of both rhHMGB1 and rsRAGE concentration for constant levels of the pair. rhS100A12 binding to rsRAGE was dependent on divalent cations (Fig. 4 and Fig. 5),

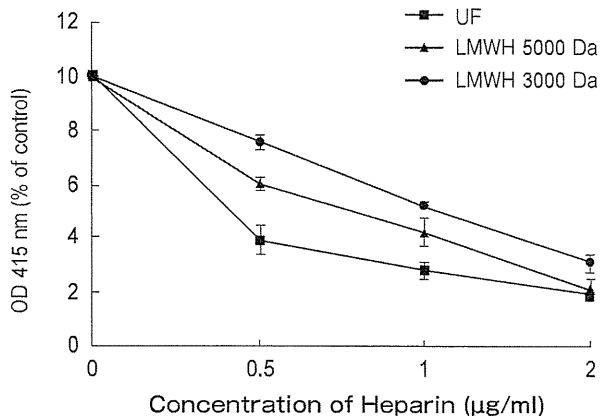

Fig. 8 Effects of heparin with different molecular sizes on rsRAGE binding to rhHMGB1. The different concentrations of UFH (■), LMWH 5000 Da (▲), and LMWH 3000 Da (●) were incubated with 25μg/ml rsRAGE for 30min at 4°C, and the mixture was added to the wells. The results were the mean ± SEM of 3 independent experiments.

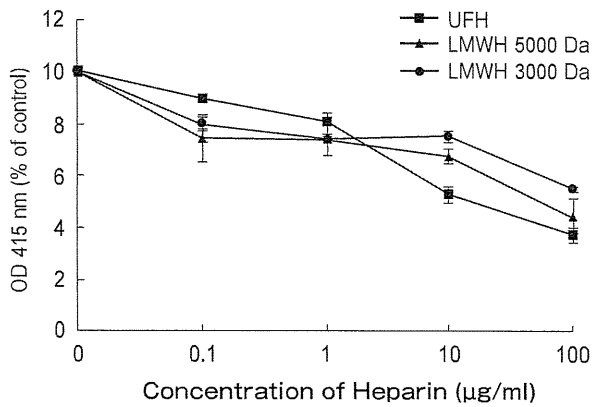

Fig. 9 Effects of heparin with different molecular sizes on rsRAGE binding to rhS100A12. The different concentration of UFH (■), LMWH 5000 Da (▲), and LMWH 3000 Da (●) were incubated with 25μg/ml rsRAGE for 30min at 4°C, and the mixture was added to the wells. The results were the mean ± SEM of 3 independent experiments.

whereas HMGB1 was not (Fig. 3). It is well known that S100A12 belongs to the EF-hand Ca^{2+} binding protein and forms a typical structure. X-ray crystallography analysis revealed both Ca^{2+} and Zn^{2+} binding sites on the structure of S100A12 [25]. The dependence of S100A12 binding to RAGE in the presence of Ca^{2+} and Zn^{2+} strongly suggested that the restrict structure of S100A12 mentioned above was required for its binding to RAGE. In contrast, rhHMGB1 binding to rsRAGE was not influenced by the presence of divalent cations. Thus, the effects of Ca^{2+} and Zn^{2+} were specific for S100A12. The binding site of HMGB1 or S100A12 on RAGE has been postulated from crystallographic studies. Hofmann *et al.* [26] suggested that S100A12 may bind to the V-domain of RAGE. On the other hand, there is controversy as to the binding site of HMGB1 on RAGE. Apparently, the affinity of HMGB1 ($K_d = 0.71\mu M$) to RAGE was higher than that of S100A12 ($K_d = 1.39\mu M$).

Since rsRAGE was able to be purified by heparin-sepharose affinity chromatography (Fig. 6), it was considered to bind to heparin, and rhS100A12 was also found to bind to heparin in the presence of Ca^{2+} (Fig. 7). By using the binding assay, we reported for the first time that heparin had inhibitory effects on the binding of rsRAGE to rhHMGB1 or rhS100A12. Dose-dependent inhibitory effects of UFH and LMWH on the binding of rsRAGE to rhHMGB1 (Fig. 8) or rhS100A12 (Fig. 9) were demonstrated. UFH is a heterogeneous mixture of polysaccharides and has been clinically used as an anticoagulant. LMWH 5000 Da is obtained through chemical or enzymatic depolymerization of UFH and shows advantages in overcoming some of the limitations associated with the use of UFH. For instance, compared with UFH, LMWH 5000 Da more potently inhibits factor Xa, an essential component of the prothrombinase complex leading to the formation of thrombin [27-30]. The exact mechanisms by which heparin blocks the binding of rhHMGB1 or rhS100A12 to rsRAGE remain unclear under this situation. Considering that HMGB1 and RAGE are all heparin-binding proteins [21, 22-24], we hypothesize that one blocking mechanism could be heparin occupancy of the binding site on rsRAGE and/or rhHMGB1. However, further experiments are necessary for the analysis of molecular interaction between rsRAGE and its ligands.

It has been suggested that heparin functions as an anti-inflammation agent by affecting some components in the inflammatory cascade, such as complement activation, platelet activating factor production [31], and expression of P- and L- selectins [32]. In addition, heparin binds antithrombin III to form a complex capable of inhibiting thrombin proteolytic activity. This inhibition prevents clot formation and allows heparin to be utilized clinically as an anticoagulant

[33]. The concept that coagulation can play a role in the inflammatory response has been well illustrated [34]. In acute inflammatory diseases, like sepsis, inflammatory and coagulation systems coexist in delicate homeostasis [35], augment each other, and combine to influence disease progression [36, 37]. Accordingly, heparin's anti-inflammatory effect may be partly assigned to its own anticoagulant property. The present results imply that another anti-inflammatory mechanism of heparin might be the interference effect on the interaction between RAGE and its ligands.

RAGE has been considered a central player in the inflammatory response [38]. It is expressed at low levels in normal tissues and in the vasculature, but becomes upregulated at sites where its ligands accumulate [39]. The RAGE axis is involved in the pathogenesis of a wide range of inflammatory disorders via the integration of ligands. HMGB1 activated Mac-1 as well as Mac-1-mediated adhesive and migratory functions of neutrophils in a RAGE-dependent manner [40]. Interaction of S100A12 with cellular RAGE on vascular endothelial cells, mononuclear phagocytes, and lymphocytes triggers cellular activation, with the expression of VCAM-1, intercellular adhesion molecule-1 (ICAM-1), and tissue factor (TF) as well as production of pro-inflammatory mediators [15]. Therefore, the interaction between RAGE and its ligands should be a target for inflammation-based disease intervention. The *in vitro* RAGE binding established in the present study will provide a convenient assay system for screening candidate drugs to interfere with the binding between RAGE and HMGB1/S100A12.

References

1. Chavakis T, Bierhaus A and Nawroth PP: RAGE (receptor for advanced glycation end products): a central player in the inflammatory response. Microbes Infect (2004) 6: 1219-1225.
2. Bierhaus A, Stern DM and Nawroth PP: RAGE in inflammation: a new therapeutic target? Curr Opin Investig Drugs (2006) 7: 985-991.
3. Schmidt AM, Vianna M, Gerlach M, Brett J, Ryan J, Kao J, Esposito C, Hegarty H, Hurley W and Clauss M: Isolation and characterization of two binding proteins for advanced glycosylation end products from bovine lung which are present on the endothelial cell surface. J Biol Chem (1992) 267: 14987-14997.
4. Dattilo BM, Fritz G, Leclerc E, Kooi CW, Heizmann CW and Chazin WJ: The extracellular region of the receptor for advanced glycation end products is composed of two independent structural units. Biochemistry (2007) 46: 6957-6970.
5. Yamagishi S, Matsui T and Nakamura K: Kinetics, role and therapeutic implications of endogenous soluble form of receptor for advanced glycation end products (sRAGE) in diabetes. Curr Drug Targets (2007) 8: 1138-1143.
6. Yamagishi S, Nakamura K and Matsui T: Advanced glycation end products (AGEs) and their receptor (RAGE) system in diabetic retinopathy. Curr Drug Discov Technol (2006) 3: 83-88.
7. Unoshima M: Therapeutic effect of anti-HMGB1 antibody and anti-RAGE anibody on SIRS/sepsis. Nippon Rinsho (2004) 62: 2323-2329 in Japanese.
8. Mruthinti S, Schade RF, Harrell DU, Gulati NK, Swamy-Mruthinti S, Lee GP and Buccafusco JJ: Autoimmunity in Alzheimer's disease as evidenced by plasma immunoreactivity against RAGE and Abeta42: complication of diabetes. Curr Alzheimer Res (2006) 3: 229-235.
9. Carroll L, Hannawi S, Marwick T and Thomas R: Rheumatoid arthritis: links with cardiovascular disease and the receptor for advanced glycation end products. Wien Med Wochenschr (2006) 156: 42-52.
10. Sisková A and Wilhelm J: Role of nonenzymatic glycation and oxidative stress on the development of complicated diabetic cataracts. Cesk Fysiol (2000) 49: 16-21 in Czech.
11. Scaffidi P, Misteli T and Bianchi ME: Release of chromatin protein HMGB1 by necrotic cells triggers inflammation. Nature (2002) 418: 191-195.
12. Abraham E, Arcaroli J, Carmody A, Wang H and Tracey KJ: HMG-1 as a mediator of acute lung inflammation. J Immunol (2000) 165: 2950-2954.
13. Zimmer DB, Cornwall EH, Landar A and Song W: The S100 protein family: history, function, and expression. Brain Res Bull (1995) 37: 417-429.
14. Vogl T, Pröpper C, Hartmann M, Strey A, Strupat K, van den Bos C, Sorg C and Roth J: S100A12 is expressed exclusively by granulocytes and acts independently from MRP8 and MRP14. J Biol Chem (1999) 274: 25291-25296.
15. Hofmann MA, Drury S, Fu C, Qu W, Taguchi A, Lu Y, Avila C, Kambham N, Bierhaus A, Nawroth P, Neurath MF, Slattery T, Beach D, McClary J, Nagashima M, Morser J, Stern D and Schmidt AM: RAGE mediates a novel proinflammatory axis: a central cell surface receptor for S100/calgranulin polypeptides. Cell (1999) 97: 889-901.
16. Alban S: Pharmacology of heparins and direct anticoagulants. Hamostaseologie (2008) 28: 400-420.
17. Tefferi A, Owen BA, Nichols WL, Witzig TE and Owen WG: Isolation of a heparin-like anticoagulant from the plasma of a patient with metastatic bladder carcinoma. Blood (1989) 74: 252-254.
18. Tyrell DJ, Kilfeather S and Page CP: Therapeutic uses of heparin beyond its traditional role as an anticoagulant. Trends Pharmacol Sci (1995) 16: 198-204.
19. Gaffney A and Gaffney P: Rheumatoid arthritis and heparin. Br J Rheumatol (1996) 35: 808-809.
20. Prajapati DN, Newcomer JR, Emmons J, Abu-Hajir M and Binion DG: Successful treatment of an acute flare of steroid-resistant Crohn's colitis during pregnancy with unfractionated heparin. Inflamm Bowel Dis (2002) 8: 192-195.
21. Myint KM, Yamamoto Y, Doi T, Kato I, Harashima A, Yonekura H, Watanabe T, Shinohara H, Takeuchi M, Tsuneyama K, Hashimoto N, Asano M, Takasawa S, Okamoto H and Yamamoto H: RAGE control of diabetic nephropathy in a mouse model: effects of RAGE gene disruption and administration of low-molecu-

lar weight heparin. Diabetes (2006) 55: 2510-2522.
22. Rauvala H and Pihlaskari R: Isolation and some characteristics of an adhesive factor of brain that enhances neurite outgrowth in central neurons. J Biol Chem (1987) 262: 16625-16635.
23. Merenmies J, Pihlaskari R, Laitinen J, Wartiovaara J and Rauvala H: 30-kDa heparin binding protein of brain (amphoterin) involved in neurite outgrowth. J Biol Chem (1991) 266: 16722-16729.
24. Rouhiainen A, Tumova S, Valmu L, Kalkkinen N and Rauvala H: Pivotal advance: analysis of proinflammatory activity of highly purified eukaryotic recombinant HMGB1 (amphoterin). J Leukoc Biol (2007) 81: 49-58.
25. Moroz OV, Antson AA, Dodson GG, Wilson KS, Skibshoj I, Lukanidin EM, Bronstein IB: Crystallization and preliminary X-ray diffraction analysis of human calcium-binding protein S100A12. Acta Crystallogr D Biol Crystallogr (2000) 56: 189-191.
26. Hofmann MA, Drury S, Fu C, Qu W, Taguchi A, Lu Y, Avila C, Kambham N, Bierhaus A, Nawroth P, Neurath MF, Slattery T, Beach D, McClary J, Nagashima M, Morser J, Stern D, Schmidt AM: RAGE mediates a novel proinflammatory axis: a central cell surface receptor for S100/calgranulin polypeptides. Cell (1999) 97: 889-901.
27. Hoppensteadt D, Walenga JM, Fareed J and Bick RL: Heparin, low-molecular-weight heparins, and heparin pentasaccharide: basic and clinical differentiation. Hematol Oncol Clin North Am (2003) 17: 313-341.
28. Spyropoulos AC: Pharmacologic therapy for the management of thrombosis: unfractionated heparin or low-molecular-weight heparin? Clin Cornerstone (2005) 7: 39-48.
29. Hoffart V, Lamprecht A, Maincent P, Lecompte T, Vigneron C and Ubrich N: Oral bioavailability of a low molecular weight heparin using a polymeric delivery system. J Control Release (2006) 113: 38-42.
30. Scheuch G, Brand P, Meyer T, Herpich C, Müllinger B, Brom J, Weidinger G, Kohlhäufl M, Häussinger K, Spannagl M, Schramm W and Siekmeier R: Anticoagulative effects of the inhaled low molecular weight heparin certoparin in healthy subjects. J Physiol Pharmacol (2007) 58 Suppl 5: 603-614.
31. Tyrrell DJ, Horne AP, Holme KR, Preuss JM and Page CP: Heparin in inflammation: potential therapeutic applications beyond anticoagulation. Adv Pharmacol (1999) 46: 151-208.
32. Wang L, Brown JR, Varki A and Esko JD: Heparin's anti-inflammatory effects require glucosamine 6-O-sulfation and are mediated by blockade of L- and P-selectins. J Clin Invest (2002) 110: 127-136.
33. Fareed J, Hoppensteadt DA and Bick RL: An update on heparins at the beginning of the new millennium. Semin Thromb Hemost (2000) 26: 5-21.
34. Esmon CT: Coagulation inhibitors in inflammation. Biochem Soc Trans (2005) 33: 401-405.
35. Schouten M, Wiersinga WJ, Levi M and van der Poll T: Inflammation, endothelium, and coagulation in sepsis. J Leukoc Biol (2008) 83: 536-545.
36. Jaimes F and de la Rosa G: Anticoagulation and sepsis: the opportunity for a new use of heparin? Biomedica (2006) 26: 150-160.
37. Okajima K: Regulation of inflammatory responses by natural anticoagulants. Immunol Rev (2001) 184: 258-274.
38. Clynes R, Moser B, Yan SF, Ramasamy R, Herold K and Schmidt AM: Receptor for AGE (RAGE): weaving tangled webs within the inflammatory response. Curr Mol Med (2007) 7: 743-751.
39. Yan SF, Ramasamy R, Naka Y and Schmidt AM: Glycation, inflammation, and RAGE: a scaffold for the macrovascular complications of diabetes and beyond. Circ Res (2003) 93: 1159-1169.
40. Orlova VV, Choi EY, Xie C, Chavakis E, Bierhaus A, Ihanus E, Ballantyne CM, Gahmberg CG, Bianchi ME, Nawroth PP and Chavakis T: A novel pathway of HMGB1-mediated inflammatory cell recruitment that requires Mac-1-integrin. EMBO J (2007) 26: 1129-1139.

European Journal of Pharmacology 623 (2009) 89–95

Contents lists available at ScienceDirect

European Journal of Pharmacology

journal homepage: www.elsevier.com/locate/ejphar

Cardiovascular Pharmacology

Histidine-rich glycoprotein inhibited high mobility group box 1 in complex with heparin-induced angiogenesis in matrigel plug assay

Hidenori Wake [a], Shuji Mori [b], Keyue Liu [a], Hideo K. Takahashi [a], Masahiro Nishibori [a,*]

[a] Department of Pharmacology, Okayama University Graduate School of Medicine, Dentistry and Pharmaceutical Sciences, Okayama 700-8558, Japan
[b] Shujitsu University, School of Pharmacy, Okayama 703-8516, Japan

ARTICLE INFO

Article history:
Received 7 May 2009
Received in revised form 28 August 2009
Accepted 8 September 2009
Available online 26 September 2009

Keywords:
Angiogenesis
HMGB1
HRG
Heparin

ABSTRACT

Histidine-rich glycoprotein (HRG) is a heparin-binding glycoprotein present in plasma at 100 μg/ml. A recent study revealed that HRG suppressed heparin-dependent basic fibroblast growth factor (bFGF)-induced angiogenesis. Additionally, we reported that high mobility group box 1 (HMGB1) in complex with heparin induces angiogenesis; therefore, we examined the effect of HRG on heparin-dependent HMGB1-induced angiogenesis in the present study. HRG completely inhibited angiogenesis induced by HMGB1 in complex with heparin. HRG inhibited the diffusion of a complex of HMGB1 with heparin from matrigel into surrounding tissue. HRG also competed with HMGB1 for heparin binding *in vitro*. Moreover, HRG inhibited heparin-dependent vascular endothelial growth factor-A_{165} (VEGF-A_{165})-induced angiogenesis. These results strongly suggested that HRG might be an inhibitor of angiogenesis induced by growth factors with heparin binding activity and that HRG may be a potential drug for angiogenic diseases, including tumor growth.

1. Introduction

Histidine-rich glycoprotein (HRG) is mainly produced in the liver and is consistently present in plasma at considerable levels (100 μg/ml, 1.25 μM) (Rylatt et al., 1981; Drasin and Sahud, 1996). HRG is an 80 kDa glycoprotein and has four domains; cystatin-like domain 1, cystatin-like domain 2, histidine–proline-rich domain and C-terminal domain. The histidine–proline-rich domain has a characteristic 12 times amino acid sequence repeat of GHHPH, whose physiological significance remains unclear (Koide et al., 1986). *In vitro* studies revealed that HRG has affinity for a variety of substances, including heparin, heparan sulfate proteoglycan (Lijnen et al., 1983; Burch et al., 1987; Peterson et al., 1987), plasminogen (Lijnen et al., 1980), thrombospnodin (Leung et al., 1984; Silverstein et al., 1985), fibrinogen, fibrin (Leung, 1986), divalent metal ions (Morgan, 1981; Guthans and Morgan, 1982), heme (Morgan, 1985) and complement C1q (Gorgani et al., 1997), suggesting that HRG may play roles relating to the control of coagulation and the fibrinolysis and immune systems; however, its functional significance has not yet been clarified. Moreover, HRG was reported to suppress vascular endothelial growth factor (VEGF) and basic fibroblast growth factor (bFGF)-induced angiogenesis, suggesting that HRG plays an important role in maintaining blood vessel homeostasis in collaboration with angiogenic growth factors (Juarez et al., 2002; Doñate et al., 2004; Guan et al., 2004; Olsson et al., 2004).

High mobility group box 1 (HMGB1) is a non-histone nuclear protein, which maintains the architecture of chromatin DNA and regulates transcription (Bustin, 1999; Yuan et al., 2004). HMGB1 is released from necrotic cells and activated macrophages. Once released into extracellular space, it acts as pro-inflammatory cytokine (Wang et al., 1999, 2001; Scaffidi et al., 2002). HMGB1 is highly expressed in inflammatory conditions, such as sepsis (Karlsson et al., 2008), rheumatic arthritis (Taniguchi et al., 2003) and atherosclerosis (Porto et al., 2006). Recent studies revealed that HMGB1 induced the sprouting and chemotaxis of vascular endothelial cells and promoted angiogenesis in the chick embryo chorioallantoic membrane (Schlueter et al., 2005; Mitola et al., 2006). Moreover, in the previous study, we demonstrated that HMGB1 complexed with heparin induced angiogenesis in a matrigel plug assay (Wake et al., 2009).

In the present study, we analyzed the effects of HRG on HMGB1-induced angiogenesis in terms of the competition for heparin binding, and the expression of tumor necrosis factor-α (TNF-α) and VEGF-A_{120}.

2. Materials and methods

2.1. Reagents

Matrigel was prepared from the Engelbreth–Holm–Swarm sarcoma inoculated in C57BL/6J mice, as previously described (Kleinman

* Corresponding author. Tel./fax: +81 86 235 7140.
E-mail address: mbori@md.okayama-u.ac.jp (M. Nishibori).

0014-2999/$ – see front matter © 2009 Elsevier B.V. All rights reserved.
doi:10.1016/j.ejphar.2009.09.010

et al., 1986). Matrigel was not supplemented with any growth factors and mainly contained laminin, collagen IV, heparan sulfate proteoglycan and entactin. Since matrigel is liquid at 4 °C and becomes a gel at 22–35 °C, we injected the ice-cold matrigel solution into the back of mice, enabling gel formation subcutaneously. Rabbit polyclonal antibody against human HRG was raised by immunization of a rabbit with human HRG purified from plasma. Rat monoclonal anti-bovine HMGB1 antibody (#10–22) was produced as previously described (Liu et al., 2007).

2.2. Animals

All animal experiments were performed in accordance with the guidelines of Okayama University on animal experiments, approved by the University's committee on animal experimentation, and conformed to the Guide for the Care and Use of Laboratory Animals published by the US National Institutes of Health (NIH Publication No. 85-23, revised 1996). Male C57BL/6J mice (24–26 g, 7–8 weeks) were obtained from the animal resources of Okayama University. Mice were housed at 22 °C and relative humidity with a regular 12-h light–dark schedule. Food and water were available *ad libitum*.

2.3. Expression and purification of recombinant human HMGB1

Recombinant human HMGB1 was produced as described previously (Wake et al., 2009). In brief, the complementary DNA (cDNA) encoding full-length HMGB1 was amplified by polymerase chain reaction (PCR) from a human microvascular endothelial cell cDNA using primers. The PCR product was subcloned into pGEX-6p-1 vector (GE Healthcare, Little Chalfont, England). The recombinant plasmids were transformed into *E. coli* strain BL21 (DE3) (Merck, San Diego, LA) and incubated overnight at 37 °C in Overnight Express Instant TB medium (Merck, San Diego, LA) to express recombinant glutathione S-transferase (GST)-HMGB1. *E. coli* extract containing GST-HMGB1 fusion proteins was incubated with glutathione-Sepharose 4B for 1 h at room temperature. After washing, the gel bed was incubated with PreScission protease for 3 h at 4 °C. After brief centrifugation, the supernatant containing GST-tag-deleted HMGB1 was collected and purified by gel filtration chromatography using TSK-gel 3000SW$_{XL}$ (Tosoh, Tokyo, Japan). Purified recombinant human HMGB1 protein was identified by Western blotting (Towbin et al., 1979) with anti-HMGB1 monoclonal antibody (#10–22). Lipopolysaccharide (LPS) content in purified recombinant human HMGB1 was less than 2.0 pg/μg protein.

2.4. Purification of HRG from human plasma

HRG was purified from human plasma, as previously described (Mori et al., 2003). In brief, human plasma was incubated with nickel-nitrilotriacetic acid (Ni-NTA) agarose (Qiagen, Hilden, Germany) for 2 h at 4 °C with gentle shaking. The gel was packed into a column and washed successively with 10 mM Tris-buffered saline (TBS) (pH 8.0) containing 10 mM imidazole, and then 10 mM Tris-buffer (TB) (pH 8.0) containing 1 M NaCl. Human HRG was eluted by 0.5 M imidazole in 10 mM TBS (pH 8.0). The protein extract was further purified by fast protein liquid chromatography (FPLC) using a Mono Q column (GE Healthcare, Little Chalfont, UK) with NaCl gradient. Purified human HRG was identified by sodium dodecyl sulfate-polyacrylamide gel electrophoresis (SDS-PAGE) and Western blotting with human HRG specific antibody.

2.5. Evaluation of angiogenesis using matrigel plug assay

Matrigel is a basement membrane component mixture and is liquid at 4 °C. Male C57BL/6J mice were anesthetized with 50% N_2O + 50% O_2, and 500 μl liquid matrigel mixture at 4 °C was injected subcutaneously into the back using a 25G needle. The matrigel mixture contained phosphate buffered saline (PBS), HMGB1 (2.5 μg/ml, 100 nM), heparin (64 units/ml) (Sigma, St. Louis, MO), HRG (100 μg/ml, 1.25 μM), heparin + HMGB1, heparin + HMGB1 + HRG, human VEGF-A_{121} (185 ng/ml, 6.5 nM) or (1.85 μg/ml, 65 nM) (Peprotech, Rocky Hill, CT), human VEGF-A_{165} (250 ng/ml, 6.5 nM) (Peprotech,), human VEGF-A_{121} + heparin, human VEGF-A_{165} + heparin, human VEGF-A_{121} + HRG, human VEGF-A_{165} + HRG, human VEGF-A_{121} + heparin + HRG or human VEGF-A_{165} + heparin + HRG. The liquid matrigel mixture solidified 5–10 min after inoculation. After 10 days, mice were sacrificed by cervical dislocation and the matrigel plugs were removed and photographed. To evaluate angiogenesis, the hemoglobin content of the removed matrigel plug was measured using a Hemoglobin B test kit (Wako, Osaka, Japan). The matrigel plug was homogenized in 10 mM PBS (pH 7.4) and centrifuged at 8000×*g* for 10 min. The supernatant was mixed with hemoglobin coloring reagent and incubated for 3 min at room temperature. Absorbance was measured at 540 nm. The total hemoglobin concentration was estimated by the standard curve using hemoglobin standard reagent. Additionally, the plugs were fixed with 10% formalin in 0.1 M phosphate buffer and stained with hematoxylin–eosin on 5 μm paraffin sections. Microvessels in the plug were assessed by CD31 immunostaining of 5 μm paraffin sections. After deparaffinization and blocking, the sections were incubated with rabbit polyclonal anti-mouse CD31 antibody (Abcam, Cambridge, UK) at 4 μg/ml followed by anti-rabbit IgG goat IgG-horseradish peroxidase (HRP) (Abcam). Immunoreactivity was visualized with 0.05% 3,3′-diaminobenzidine (Sigma) and 0.03% H_2O_2. Nuclei were counterstained with Mayer's hematoxylin. A negative control for immunohistochemical staining was obtained with the same concentration of normal rabbit IgG. The number of CD31-positive vessels was counted in 5 fields of the matrigel plug section under a microscope at 400× magnification. Microvessel density (MVD) was expressed as the number of microvessels per square millimeter.

2.6. Competition between HMGB1 and HRG using heparin-binding plate

Heparin (5 units/ml) in 10 mM PBS (pH 7.4) was added to a heparin binding plate (BD, Franklin Lakes, NJ). After three washings with acetate buffer (100 mM NaCl, 50 mM NaAc, 0.2% Tween-20 pH 7.2), 0.2% gelatin solution (Sigma) was added to wells to block nonspecific binding. Each concentration of HMGB1 (0, 5 and 10 μg/ml) and HRG (0, 10, 50 and 100 μg/ml) was added to the well and incubated at 37 °C for 2 h. After washing, 0.5 μg/ml anti-HMGB1 monoclonal antibody (R&D Systems, Minneapolis, MN) was added to wells followed by the addition of anti-mouse IgG goat polyclonal IgG-HRP (MBL, Nagoya, Japan) to determine bound HMGB1. The reaction was developed by ABTS and H_2O_2 and determined at 405 nm using a microplate reader model 680 (Bio-rad, Hercules, CA).

2.7. Western blot analysis of HMGB1 levels in matrigel plug

Matrigel mixture that contained PBS, HMGB1 (2.5 μg/ml, 100 nM), heparin (64 units/ml) + HMGB1 or heparin + HMGB1 + HRG (100 μg/ml, 1.25 μM) was injected subcutaneously into the back. After 1, 3 or 10 days, mice were sacrificed and the matrigel plugs were removed. Equal amounts of matrigel homogenate sample corresponding to 2.5 mg wet weight were electrophoresed on polyacrylamide gel (12.5%) and transferred onto a polyvinylidine difloride (PVDF) membrane (Bio-rad). After the membrane was stained with Ponceau S, it was blocked with 10% skim milk for 1 h and incubated overnight at 4 °C with mouse monoclonal anti-human HMGB1 antibody (R&D Systems) followed by anti-mouse IgG goat polyclonal IgG-HRP (MBL, Nagoya, Japan) for 1 h at room temperature. The signals were finally visualized using the enhanced chemiluminescence system (Pierce Biotechnology, Rockford, IL).

2.8. Reverse transcription polymerase chain reaction (RT-PCR)

Mouse skin samples in contact with matrigels were dissected from the portion just above the gels as 5 mm square. Total RNA was purified from the skin sample using an RNeasy fibrous tissue mini kit (Qiagen, Hilden, Germany) and cDNA was synthesized using Takara RNA PCR kit Ver. 3.0 (Takara Bio, Nagahama, Japan) according to the manufacturer's instructions. PCR was performed in a PCR Thermal Cycler (Takara Bio) using Ex Taq DNA polymerase HS (Takara Bio), and sequence-specific primers according to the conditions described previously (Wake et al., 2009). The PCR product was electrophoresed on 2% agarose gel.

2.9. Real-time quantitative PCR

Real-time PCR was performed with a Light Cycler (Roche, Basel, Swiss) using SYBR premix Ex Taq (Takara Bio, Shiga, Japan) and cDNA from mouse skin and sequence-specific primers (Wake et al., 2009), according to the manufacturer's instructions. The expression of glyceraldehyde-3-phospate dehydrogenase (GAPDH) was used to normalize cDNA levels. The PCR products were analyzed by a melting curve to ascertain the specificity of amplification.

2.10. Statistical analysis

For each experiment, data are presented as the means ± S.E.M. The results were analyzed by one-way analysis of variance (one-way ANOVA) followed by Student's *t*-test. *P* values < 0.05 were considered significant.

3. Results

3.1. Effect of HRG on HMGB1-induced angiogenesis in the presence of heparin using matrigel plug assay

We investigated the anti-angiogenic effects of HRG on HMGB1-induced angiogenesis in the presence of heparin using a matrigel plug assay. Matrigel mixture was implanted subcutaneously into the back. After 10 days, the matrigel plugs were removed. The matrigel plug treated with PBS, HMGB1 or HRG alone was pale in color, whereas the matrigel plug treated with heparin alone was slightly red; however, the matrigel plug treated with a combination of HMGB1 and heparin was very red and the hemoglobin content of this plug was significantly increased, indicating that HMGB1-induced angiogenesis was heparin-dependent. The addition of HRG to the combination of HMGB1 and heparin almost completely inhibited the increase in hemoglobin content induced by the combination (Fig. 1A, B). A thin section of matrigel was stained with hematoxylin–eosin and anti-CD31 antibody. In the group treated with a combination of HMGB1 and heparin, CD31-positive luminal structures and many infiltrating cells, including leukocytes, were observed in the plug (Fig. 2A panels e, k); however, a few CD31-positive structures and infiltrating cells in the gel were observed in sections from other groups (Fig. 2A panels a–d, f, g–j, l). The number of CD31-positive microvessels was counted in five random fields. In the plug treated with the combination of HMGB1 and heparin, CD31-positive microvessels were significantly increased compared to those by HMGB1, heparin and HRG alone. HRG completely inhibited the increase in CD31-positive microvessels induced by the combination. There was a significant correlation between the hemoglobin contents and the number of CD31-positive microvessels. Collectively, it was suggested that HRG inhibited the migration activity of vascular endothelial cells as well as leukocytes induced by the combination of HMGB1 and heparin (Fig. 2B).

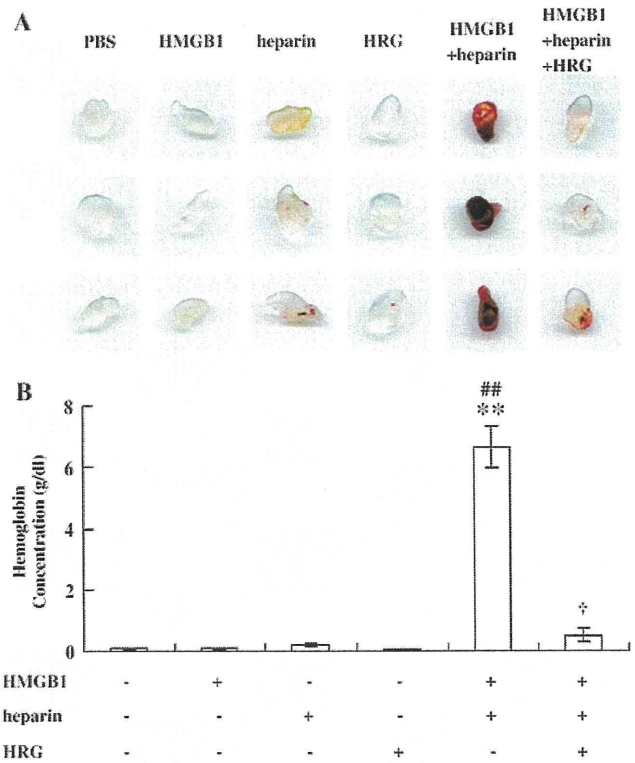

Fig. 1. Effect of HRG on the angiogenesis induced by HMGB1 and heparin using matrigel assay. (A) Matrigel mixture contained HMGB1, HRG and heparin alone or in combination. Ten days after inoculation, the matrigel plugs were recovered. Each group consisted of 6 mice. (B) Hemoglobin content in matrigel plugs was determined. Data are the means ± S.E.M. of 6 matrigels. $^{**}P<0.01$ *vs.* PBS control; $^{\#\#}P<0.01$ *vs.* heparin alone; $^{\dagger}P<0.05$ *vs.* combination of HMGB1 and heparin.

3.2. Competition between HRG and HMGB1 for heparin binding

To evaluate the inhibitory effect of HRG on HMGB1–heparin binding, we performed a competitive binding assay using a heparin-binding plate. The molar ratios of HRG/HMGB1, ranging from 0.3 to 6.3, were examined. The addition of increasing concentrations of HRG inhibited HMGB1–heparin binding in a concentration-dependent manner. One hundred micrograms/milliliter HRG (normal human plasma concentration) inhibited HMGB1 (5 μg/ml: twice the concentration of HMGB1 in matrigel plug assay)–heparin binding by 75% (Fig. 3).

3.3. Determination of HMGB1 levels in matrigel

To identify the degradation of HMGB1 in matrigel and its diffusion from gel, we detected HMGB1 in plugs recovered 1, 3 and 10 days after inoculation using Western blot analysis. Each matrigel mixture contained PBS, HMGB1, heparin + HMGB1 and heparin + HMGB1 + HRG, respectively. The same amount of matrigel homogenate was loaded onto each lane (Fig. 4A). In each matrigel plug recovered 1 day after inoculation, a constant level of HMGB1 was detected. After 3 days, HMGB1 was completely ablated in matrigel with HMGB1 and heparin. Such a disappearance was completely suppressed by the addition of HRG. HMGB1 levels did not significantly change in matrigel during a 10-day period except for HMGB1 and heparin groups (Fig. 4B). Moreover, no degradative bands were detected in each group throughout the period. These data suggested that HMGB1 in complex with heparin diffused into tissue surrounding matrigel and HRG completely suppressed its diffusion.

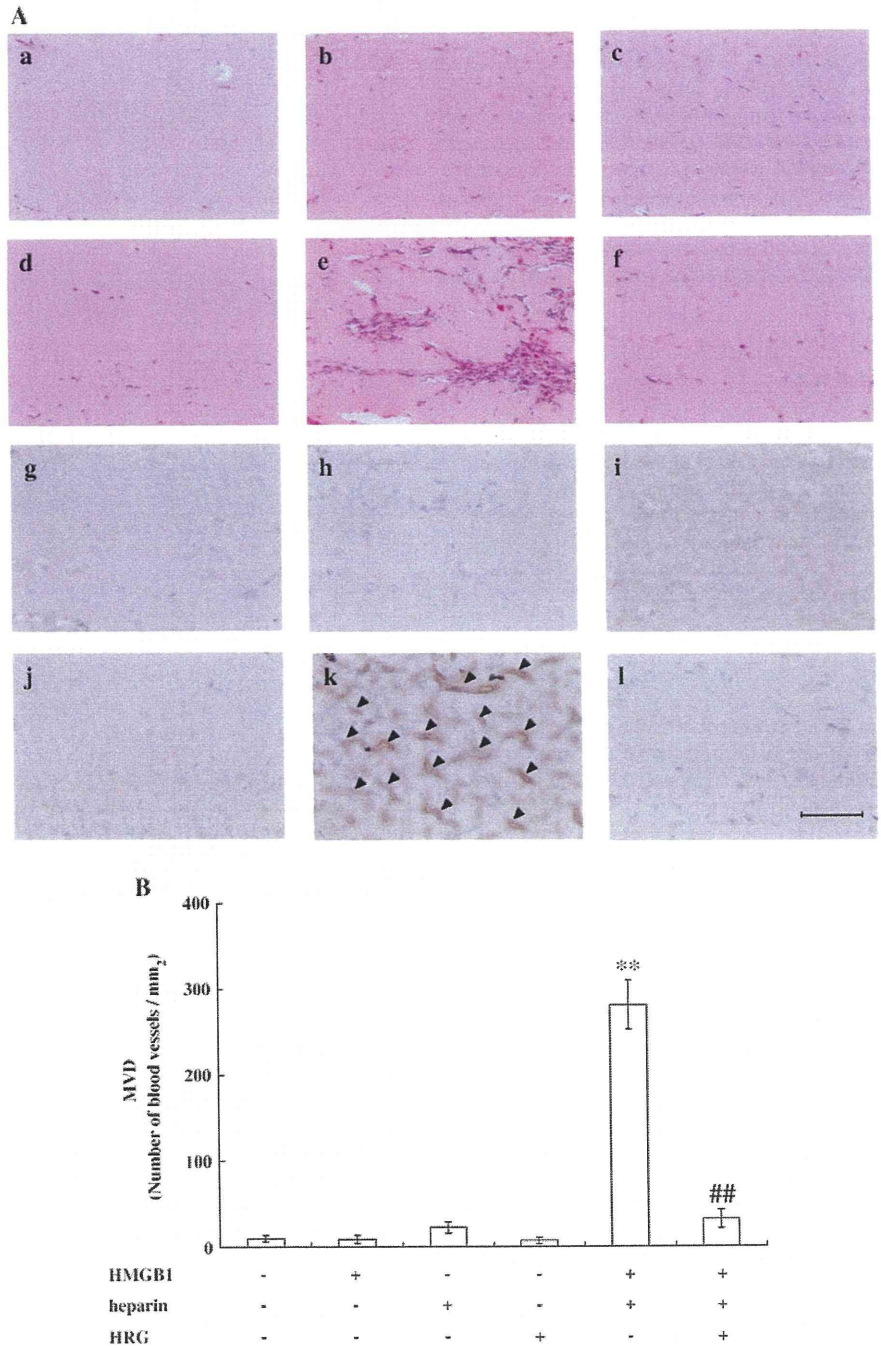

Fig. 2. Histological study of matrigel plug sections. (A) Matrigel plug sections were stained by hematoxylin–eosin (a–f) or by anti-CD31 antibody (g–l). Matrigels contained PBS (a,g), HMGB1 alone (b,h), heparin alone (c,i), HRG alone (d,j), a combination of HMGB1 and heparin (e,k), a combination of HMGB1, heparin and HRG (f,l). *Arrowheads* indicate CD31-positive blood vessels. Scale bar represents 100 μm. (B) Under a microscope, CD31-positive vessels were counted in 5 fields of a matrigel plug section at 400× magnification. Microvessel density (MVD) was expressed as the number of microvessels per square millimeter. Data are the means ± S.E.M. of 5 fields. $^{**}P<0.01$ *vs.* PBS control group. $^{\#\#}P<0.01$ *vs.* combination of HMGB1 and heparin.

3.4. HRG inhibited the expression of TNF-α and VEGF-A_{120} induced by the combination of HMGB1 and heparin

Ten days after inoculation of matrigel, total RNA was extracted from mouse skin surrounding matrigel. The expression of messenger RNA (mRNA) coding for cytokines, matrix metalloproteinases (MMPs) or growth factors was determined by RT-PCR. Treatment with a combination of HMGB1 and heparin significantly up-regulated the expressions of TNF-α and VEGF-A_{120} in mouse skin surrounding matrigel as compared with any groups receiving treatment with PBS, heparin, HMGB1 and HRG alone. The addition of HRG to the combination of HMGB1 and heparin abolished the enhanced expression of TNF-α and VEGF-A_{120} completely (Fig. 5A). In contrast, there were no significant differences in inducible nitric oxide synthase (iNOS), endothelial NOS (eNOS), MMP-2, MMP-9, VEGF receptor-1 (VEGFR-1), VEGFR-2, VEGF-A_{164}, VEGF-A_{188} and bFGF mRNA levels among groups (data not shown). The expression of TNF-α and VEGF-A_{120} mRNA was quantified using real-time PCR. Treatment of HMGB1 alone significantly increased the expression of

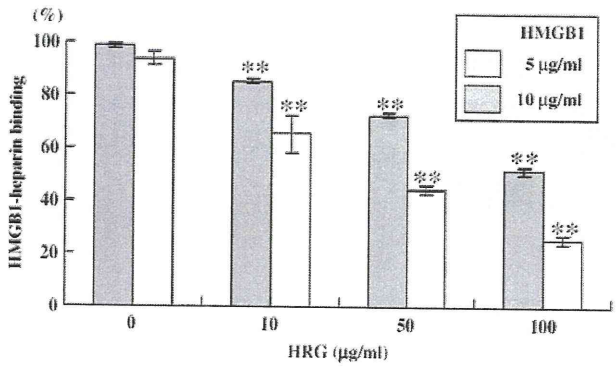

Fig. 3. HMGB1 binding to heparin. HMGB1 alone or in combination with indicated concentrations of HRG (10, 50 or 100 μg/ml) was added to heparin-coated wells of heparin binding plate and incubation continued for 2 h at 37 °C. Bound HMGB1 was detected with anti-HMGB1 monoclonal antibody, followed by anti-mouse IgG-HRP. Data are the means ± S.E.M. of 3 wells. $^{**}P<0.01$ *vs.* HMGB1 alone.

TNF-α mRNA compared with the PBS-alone group. TNF-α and VEGF-A_{120} mRNA levels were significantly increased in the group treated with the combination of HMGB1 and heparin compared with groups treated with PBS, heparin, HMGB1 and HRG alone. The addition of HRG suppressed the enhanced expression of TNF-α and VEGF-A_{120} mRNA induced by the combination of HMGB1 and heparin (Fig. 5B).

3.5. Effects of VEGF, HRG and heparin on angiogenesis using matrigel plug assay

We assessed the anti-angiogenic effects of HRG on VEGF-induced angiogenesis using the matrigel plug assay. Ten days after inoculation, the matrigel plugs were recovered. VEGF-A_{165} (250 ng/ml, 6.5 nM), a heparin binding growth factor, alone did not induce angiogenesis (Fig. 6), whereas the combination of VEGF-A_{165} and heparin did induce angiogenesis (Fig. 6). Angiogenesis induced by VEGF-A_{165} and heparin was suppressed by HRG, as in the combination of HMGB1 and heparin. VEGF-A_{121} (185 ng/ml, 6.5 nM) lacking the heparin-binding domain alone and the combination of VEGF-A_{121} and heparin did not induce angiogenesis significantly. These results suggested that heparin has an important role in VEGF-induced angiogenesis.

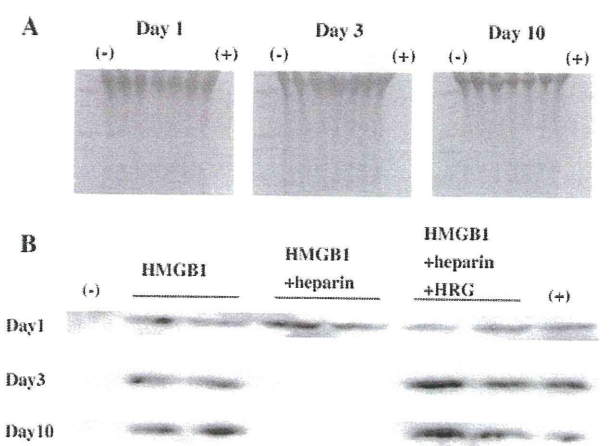

Fig. 4. Determination of HMGB1 levels in matrigel using Western blot analysis matrigel mixture contained PBS, HMGB1, heparin + HMGB1 or heparin + HMGB1 + HRG. After 1, 3 and 10 days, the matrigel plugs were recovered. Matrigel plug homogenate corresponding to 2.5 mg wet weight of matrigel was loaded onto each lane. (A) Ponseau S staining of PVDF membrane. (B) Detection of HMGB1 in matrigel. (−) Negative control, matrigel contains PBS alone. (+) Positive control, recombinant human HMGB1.

4. Discussion

In the previous study, we reported that HMGB1 in complex with heparin induced marked angiogenesis in the matrigel plug assay (Wake et al., 2009). One of the main reasons for heparin dependence of the angiogenic effect of HMGB1 was demonstrated to be due to the diffusibility of HMGB1 and heparin complex from matrigel into surrounding tissue where the proliferation of infiltrating microvasculature occurred (Wake et al., 2009). It was speculated that the restriction of diffusion of HMGB1 alone was ascribed to the binding of HMGB1 to the abundant heparan sulfate proteoglycan structure in matrigel. The other reason may be the resistance of HMGB1 and heparin complex to degradation by proteases (Wake et al., 2009). Collectively, HMGB1 in complex with heparin can diffuse to surrounding matrigel and stimulate vascular endothelial cells without degradation by proteases. Consistent with these findings, HMGB1 in combination with heparin induced the expression of TNF-α and VEGF-A_{120} mRNA. Since it is known that both TNF-α and VEGF-A_{120} have angiogenic activities (Leibovich et al., 1987; Yoshida et al., 1997; Hoeben et al., 2004), the present result implies that HMGB1 release may occur upstream of TNF-α and VEGF-A_{120} production under some *in vivo* conditions. Moreover, VEGF-A_{165}, heparin-binding growth factor, in complex with heparin, induced angiogenesis. This revealed that heparin has an important role in heparin-binding growth factor-induced angiogenesis.

In the present study, HRG completely inhibited the angiogenesis induced by HMGB1 and heparin complex. Because HRG was also reported to interact strongly with heparin (K_d~7 nM) (Lijnen et al., 1983), we examined the competition between HMGB1 and HRG for heparin binding (Fig. 3). The results suggested that HMGB1 and HRG have similar affinity for heparin and are competitive for heparin binding under a constant level of heparin; therefore, it is quite likely that the addition of HRG to matrigel replaced the binding of HMGB1 to heparin, facilitating the trapping of HMGB1 by heparan sulfate proteoglycan in matrigel. This notion was strongly supported by the determination of HMGB1 levels in matrigel under different conditions. Additionally, HRG is known to inhibit the digestion of heparan sulfate by heparanase released from macrophages and mast cells (Freeman and Parish, 1997), thereby inhibiting the de-anchoring of HMGB1 from extracellular matrix (ECM). Parallel and complete inhibitory effects of HRG on both angiogenesis and the expression of TNF-α and VEGF-A_{120} induced by the combination of HMGB1 and heparin strongly suggested that the limitation of HMGB1 diffusion, suppression of TNF-α and VEGF-A_{120} expression and inhibition of angiogenesis were causative and successive events in this matrigel assay system. In the present study, we also demonstrated that HRG inhibited the heparin-dependent effect of VEGF-A_{165} with the heparin-binding domain on angiogenesis. Moreover, it was reported that HRG inhibited the heparin-dependent effect of bFGF on angiogenesis (Juarez et al., 2002; Guan et al., 2004). These findings as a whole suggest that HRG may be a common inhibitor of heparin-binding growth factors.

HMGB1 was reported to be released from necrotic cells. HMGB1 has multiple pro-inflammatory effects on vascular endothelial cells as well as leucocytes. In addition, the present study confirmed the heparin-dependent angiogenic activity of HMGB1; therefore, it is speculated that the release of heparin from mast cells at a certain stage of inflammation may trigger angiogenic activity by de-anchoring the extracellular HMGB1 trapped by heparan sulfate in ECM or on the cell surface. Furthermore, the subsequent exposure of HMGB1–heparin complex to a relatively high concentration of HRG in plasma after canalization will arrest angiogenesis by competing heparin binding. Thus, HRG may also regulate the angiogenic activity of multiple factors, including HMGB1.

It was reported that many types of cancer cells release HMGB1 (Kawahara et al., 1996; Taguchi et al., 2000; Choi et al., 2003; Kuniyasu et al., 2003, 2004) and that mast cells with heparin-containing granules are abundant in the invasive front of tumors (Yoshii et al., 2005; Halin

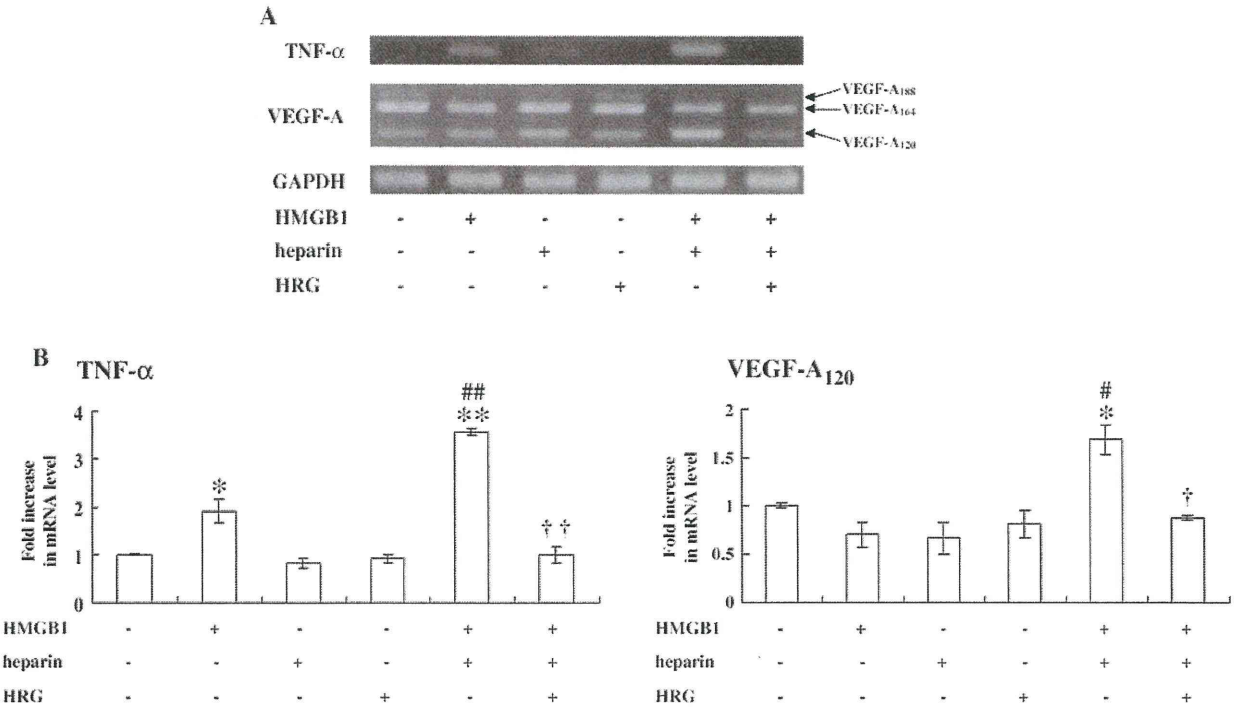

Fig. 5. Expression of mRNAs in mouse skin surrounding matrigel plug. (A) The expression of mRNA in mouse skin surrounding matrigel was determined by RT-PCR. Ten days after inoculation with matrigel, total RNA was extracted from mouse skin surrounding matrigel. Representative results from 3 mice are shown. (B) The expression of TNF-α and VEGF-A_{120} in mouse skin surrounding the matrigel plug was quantified using real-time PCR. The expression of GAPDH was used to normalize cDNA levels. Data are the means ± S.E.M. of 3 animals. $^{*}P<0.05$, $^{**}P<0.01$ *vs.* control group; $^{\#\#}P<0.01$ *vs.* combination of HMGB1 and heparin.

et al., 2009); therefore, it is possible that part of the angiogenic activity of the invasive front of tumors may be ascribed to the action of HMGB1 and heparin complex. HRG not only inhibits VEGF- and bFGF-induced angiogenesis in the presence of heparin but also suppresses tumor growth (Juarez et al., 2002; Doñate et al., 2004; Guan et al., 2004; Olsson et al., 2004). These findings imply that HRG or HRG-derived active

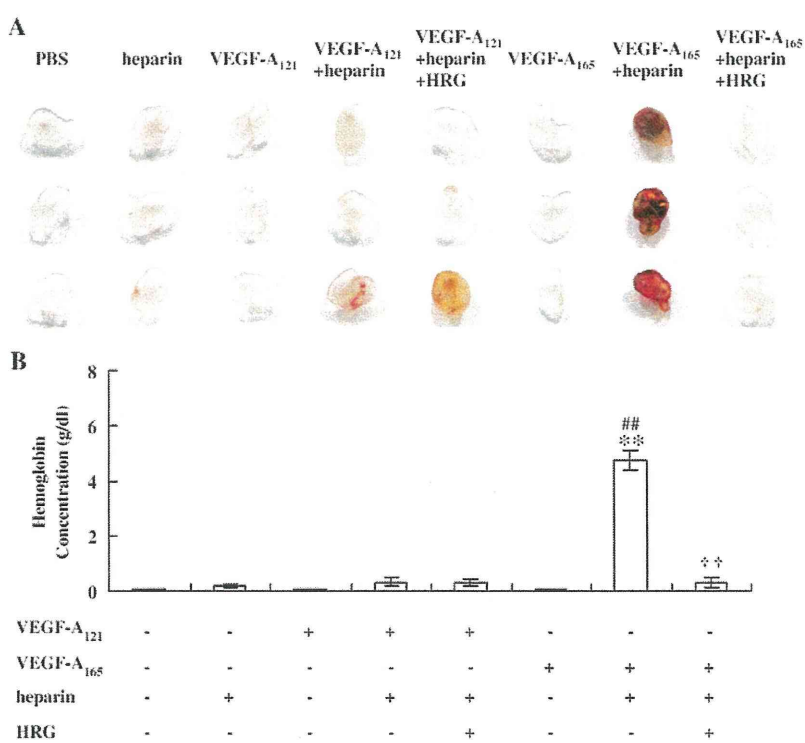

Fig. 6. Effect of HRG on angiogenesis induced by VEGF using matrigel. (A) Matrigel mixture contained VEGF-A_{121}, VEGF-A_{165}, HRG and heparin alone or in combination. Ten days after inoculation, the matrigel plugs were recovered. Each group consisted of 6 mice. (B) Hemoglobin contents in matrigel plugs were determined. Data are the means ± S.E.M. of 6 matrigels. $^{**}P<0.01$ *vs.* PBS control without treatment. $^{\#\#}P<0.01$ *vs.* heparin alone. $^{\dagger\dagger}P<0.01$ *vs.* combination of VEGF-A_{165} and heparin.

domain peptides may have high potential for cancer therapy. Further work is necessary on this issue.

Acknowledgements

This work was supported in part by grants-in-aid for scientific research from the Japan Foundation of Cardiovascular Research to H.W., from the Japan Society for the Promotion of Science (JSPS No. 21390071 and JSPS No. 21659141) to M.N. and (JSPS No. 21590594) to K.L. and from Mitsui Sumitomo Insurance Welfare Foundation to S.M.

References

Burch, M.K., Blackburn, M.N., Morgan, W.T., 1987. Further characterization of the interaction of histidine-rich glycoprotein with heparin: evidence for the binding of two molecules of histidine-rich glycoprotein by high molecular weight heparin and for the involvement of histidine residues in heparin binding. Biochemistry 26, 7477–7482.

Bustin, M., 1999. Regulation of DNA-dependent activities by the functional motifs of the high-mobility-group chromosomal proteins. Mol. Cell. Biol. 19, 5237–5246.

Choi, Y.R., Kim, H., Kang, H.J., Kim, N.G., Kim, J.J., Park, K.S., Paik, Y.K., Kim, H.O., Kim, H., 2003. Overexpression of high mobility group box 1 in gastrointestinal stromal tumors with KIT mutation. Cancer Res. 63, 2188–2193.

Doñate, F., Juarez, J.C., Guan, X., Shipulina, N.V., Plunkett, M.L., Tel-Tsur, Z., Shaw, D.E., Morgan, W.T., Mazar, A.P., 2004. Peptides derived from the histidine–proline domain of the histidine–proline-rich glycoprotein bind to tropomyosin and have antiangiogenic and antitumor activities. Cancer Res. 64, 5812–5817.

Drasin, T., Sahud, M., 1996. Blood-type and age affect human plasma levels of histidine-rich glycoprotein in a large population. Thromb. Res. 84, 179–188.

Freeman, C., Parish, C.R., 1997. A rapid quantitative assay for the detection of mammalian heparanase activity. Biochem. J. 325, 229–237.

Gorgani, N.N., Parish, C.R., Easterbrook, Smith, S.B., Altin, J.G., 1997. Histidine-rich glycoprotein binds to human IgG and C1q and inhibits the formation of insoluble immune complexes. Biochemistry 36, 6653–6662.

Guan, X., Juarez, J.C., Qi, X., Shipulina, N.V., Shaw, D.E., Morgan, W.T., McCrae, K.R., Mazar, A.P., Doñate, F., 2004. Histidine–proline rich glycoprotein (HPRG) binds and transduces anti-angiogenic signals through cell surface tropomyosin on endothelial cells. Thromb. Haemost. 92, 403–412.

Guthans, S.L., Morgan, W.T., 1982. The interaction of zinc, nickel and cadmium with serum albumin and histidine-rich glycoprotein assessed by equilibrium dialysis and immunoadsorbent chromatography. Arch. Biochem. Biophys. 218, 320–328.

Halin, S., Rudolfsson, S.H., Van Rooijen, N., Bergh, A., 2009. Extratumoral macrophages promote tumor and vascular growth in an orthotopic rat prostate tumor model. Neoplasia 11, 177–186.

Hoeben, A., Landuyt, B., Highley, M.S., Wildiers, H., Van Oosterom, A.T., De Bruijn, E.A., 2004. Vascular endothelial growth factor and angiogenesis. Pharmacol. Rev. 56, 549–580.

Juarez, J.C., Guan, X., Shipulina, N.V., Plunkett, M.L., Parry, G.C., Shaw, D.E., Zhang, J.C., Rabbani, S.A., McCrae, K.R., Mazar, A.P., Morgan, W.T., Doñate, F., 2002. Histidine–proline-rich glycoprotein has potent antiangiogenic activity mediated through the histidine–proline-rich domain. Cancer Res. 62, 5344–5350.

Karlsson, S., Pettilä, V., Tenhunen, J., Laru-Sompa, R., Hynninen, M., Ruokonen, E., 2008. HMGB1 as a predictor of organ dysfunction and outcome in patients with severe sepsis. Intensive Care Med. 34, 1046–1053.

Kawahara, N., Tanaka, T., Yokomizo, A., Nanri, H., Ono, M., Wada, M., Kohno, K., Takenaka, K., Sugimachi, K., Kuwano, M., 1996. Enhanced coexpression of thioredoxin and high mobility group protein 1 genes in human hepatocellular carcinoma and the possible association with decreased sensitivity to cisplatin. Cancer Res. 56, 5330–5333.

Kleinman, H.K., McGarvey, M.L., Hassell, J.R., Star, V.L., Cannon, F.B., Laurie, G.W., Martin, G.R., 1986. Basement membrane complexes with biological activity. Biochemistry 25, 312–318.

Koide, T., Foster, D., Yoshitake, S., Davie, E.W., 1986. Amino acid sequence of human histidine-rich glycoprotein derived from the nucleotide sequence of its cDNA. Biochemistry 25, 2220–2225.

Kuniyasu, H., Chihara, Y., Kondo, H., 2003. Differential effects between amphoterin and advanced glycation end products on colon cancer cells. Int. J. Cancer 104, 722–727.

Kuniyasu, H., Sasaki, T., Sasahira, T., Ohmori, H., Takahashi, T., 2004. Depletion of tumor-infiltrating macrophages is associated with amphoterin expression in colon cancer. Pathobiology 71, 129–136.

Leibovich, S.J., Polverini, P.J., Shepard, H.M., Wiseman, D.M., Shively, V., Nuseir, N., 1987. Macrophage-induced angiogenesis is mediated by tumour necrosis factor-alpha. Nature 329, 630–632.

Leung, L.L., Nachman, R.L., Harpel, P.C., 1984. Complex formation of platelet thrombospondin with histidine-rich glycoprotein. J. Clin. Invest. 73, 5–12.

Leung, L.L., 1986. Interaction of histidine-rich glycoprotein with fibrinogen and fibrin. J. Clin. Invest. 77, 1305–1311.

Lijnen, H.R., Hoylaerts, M., Collen, D., 1980. Isolation and characterization of a human plasma protein with affinity for the lysine binding sites in plasminogen. Role in the regulation of fibrinolysis and identification as histidine-rich glycoprotein. J. Biol. Chem. 255, 10214–10222.

Lijnen, H.R., Hoylaerts, M., Collen, D., 1983. Heparin binding properties of human histidine-rich glycoprotein. Mechanism and role in the neutralization of heparin in plasma. J. Biol. Chem. 258, 3803–3808.

Liu, K., Mori, S., Takahashi, H.K., Tomono, Y., Wake, H., Kanke, T., Sato, Y., Hiraga, N., Adachi, N., Yoshino, T., Nishibori, M., 2007. Anti-high mobility group box 1 monoclonal antibody ameliorates brain infarction induced by transient ischemia in rats. FASEB J. 21, 3904–3916.

Mitola, S., Belleri, M., Urbinati, C., Coltrini, D., Sparatore, B., Pedrazzi, M., Melloni, E., Presta, M., 2006. Cutting edge: extracellular high mobility group box-1 protein is a proangiogenic cytokine. J. Immunol. 176, 12–15.

Morgan, W.T., 1981. Interactions of the histidine-rich glycoprotein of serum with metals. Biochemistry 20, 1054–1061.

Morgan, W.T., 1985. The histidine-rich glycoprotein of serum has a domain rich in histidine, proline, and glycine that binds heme and metals. Biochemistry 24, 1496–1501.

Mori, S., Takahashi, H.K., Yamaoka, K., Okamoto, M., Nishibori, M., 2003. High affinity binding of serum histidine-rich glycoprotein to nickel-nitrilotriacetic acid: the application to microquantification. Life Sci. 73, 93–102.

Olsson, A.K., Larsson, H., Dixelius, J., Johansson, I., Lee, C., Oellig, C., Björk, I., Claesson-Welsh, L., 2004. A fragment of histidine-rich glycoprotein is a potent inhibitor of tumor vascularization. Cancer Res. 64, 599–605.

Peterson, C.B., Morgan, W.T., Blackburn, M.N., 1987. Histidine-rich glycoprotein modulation of the anticoagulant activity of heparin. Evidence for a mechanism involving competition with both antithrombin and thrombin for heparin binding. J. Biol. Chem. 262, 7567–7574.

Porto, A., Palumbo, R., Pieroni, M., Aprigliano, G., Chiesa, R., Sanvito, F., Maseri, A., Bianchi, M.E., 2006. Smooth muscle cells in human atherosclerotic plaques secrete and proliferate in response to high mobility group box 1 protein. FASEB J. 20, 2565–2566.

Rylatt, D.B., Sia, D.Y., Mundy, J.P., Parish, C.R., 1981. Autorosette inhibition factor: isolation and properties of the human plasma protein. Eur. J. Biochem. 119, 641–646.

Scaffidi, P., Misteli, T., Bianchi, M.E., 2002. Release of chromatin protein HMGB1 by necrotic cells triggers inflammation. Nature 418, 191–195.

Schlueter, C., Weber, H., Meyer, B., Rogalla, P., Röser, K., Hauke, S., Bullerdiek, J., 2005. Angiogenetic signaling through hypoxia: HMGB1: an angiogenetic switch molecule. Am. J. Pathol. 166, 1259–1263.

Silverstein, R.L., Leung, L.L., Harpel, P.C., Nachman, R.L., 1985. Platelet thrombospondin forms a trimolecular complex with plasminogen and histidine-rich glycoprotein. J. Clin. Invest. 75, 2065–2073.

Taguchi, A., Blood, D.C., del Toro, G., Canet, A., Lee, D.C., Qu, W., Tanji, N., Lu, Y., Lalla, E., Fu, C., Hofmann, M.A., Kislinger, T., Ingram, M., Lu, A., Tanaka, H., Hori, O., Ogawa, S., Stern, D.M., Schmidt, A.M., 2000. Blockade of RAGE-amphoterin signalling suppresses tumour growth and metastases. Nature 405, 354–360.

Taniguchi, N., Kawahara, K., Yone, K., Hashiguchi, T., Yamakuchi, M., Goto, M., Inoue, K., Yamada, S., Ijiri, K., Matsunaga, S., Takajima, T., Komiya, S., Maruyama, I., 2003. High mobility group box chromosomal protein 1 plays a role in the pathogenesis of rheumatoid arthritis as a novel cytokine. Arthritis Rheum. 48, 971–981.

Towbin, H., Staehelin, T., Gordon, J., 1979. Electrophoretic transfer of proteins from polyacrylamide gels to nitrocellulose sheets: procedure and some applications. Proc. Natl. Acad. Sci. U. S. A. 76, 4350–4354.

Wake, H., Mori, S., Liu, K., Takahashi, H.K., Nishibori, M., 2009. High mobility group box 1 complexed with heparin induced angiogenesis in matrigel plug assay. Acta Med. Okayama. 63, 249–262.

Wang, H., Bloom, O., Zhang, M., Vishnubhakat, J.M., Ombrellino, M., Che, J., Frazier, A., Yang, H., Ivanova, S., Borovikova, L., Manogue, K.R., Faist, E., Abraham, E., Andersson, J., Andersson, U., Molina, P.E., Abumrad, N.N., Sama, A., Tracey, K.J., 1999. HMG-1 as a late mediator of endotoxin lethality in mice. Science 285, 248–251.

Wang, H., Yang, H., Czura, C.J., Sama, A.E., Tracey, K.J., 2001. HMGB1 as a late mediator of lethal systemic inflammation. Am. J. Respir. Crit. Care Med. 164, 1768–1773.

Yoshida, S., Ono, M., Shono, T., Izumi, H., Ishibashi, T., Suzuki, H., Kuwano, M., 1997. Involvement of interleukin-8, vascular endothelial growth factor, and basic fibroblast growth factor in tumor necrosis factor alpha-dependent angiogenesis. Mol. Cell. Biol. 17, 4015–4023.

Yoshii, M., Jikuhara, A., Mori, S., Iwagaki, H., Takahashi, H.K., Nishibori, M., Tanaka, N., 2005. Mast cell tryptase stimulates DLD-1 carcinoma through prostaglandin- and MAP kinase-dependent manners. J. Pharmacol. Sci. 98, 450–458.

Yuan, F., Gu, L., Guo, S., Wang, C., Li, G.M., 2004. Evidence for involvement of HMGB1 protein in human DNA mismatch repair. J. Biol. Chem. 279, 20935–20940.

0022-3565/09/3312-656–670$20.00
THE JOURNAL OF PHARMACOLOGY AND EXPERIMENTAL THERAPEUTICS
JPET 331:656–670, 2009

Vol. 331, No. 2
157594/3527560
Printed in U.S.A.

Prostaglandin E_2 Inhibits Advanced Glycation End Product-Induced Adhesion Molecule Expression, Cytokine Production, and Lymphocyte Proliferation in Human Peripheral Blood Mononuclear Cells

Hideo Kohka Takahashi, Keyue Liu, Hidenori Wake, Shuji Mori, Jiyong Zhang, Rui Liu, Tadashi Yoshino, and Masahiro Nishibori

Departments of Pharmacology (H.K.T., K.L., H.W., J.Z., R.L., M.N.) and Pathology (T.Y.), Okayama University Graduate School of Medicine, Dentistry, and Pharmaceutical Sciences, Okayama, Japan; and Department of Pharmacy, Shujitsu University, Okayama, Japan (S.M.)

Received June 11, 2009; accepted August 20, 2009

ABSTRACT

Advanced glycation end product (AGE) subtypes, proteins or lipids that become glycated after exposure to sugars, induce complications in diabetes. Among the various AGE subtypes, glyceraldehyde-derived AGE (AGE-2) and glycolaldehyde-derived AGE (AGE-3) have been indicated to play roles in inflammation in diabetic patients. The engagement of AGEs and receptor for AGEs activates monocytes. Because the engagement of intercellular adhesion molecule-1 (ICAM-1), B7.1, B7.2, and CD40 on monocytes with their ligands on T cells plays roles in cytokine production, we investigated the effects of AGE-2 and AGE-3 on the expressions of ICAM-1, B7.1, B7.2, and CD40 on monocytes, the production of interferon γ and tumor necrosis factor α, and the lymphocyte proliferation in human peripheral blood mononuclear cells and their modulation by prostaglandin E_2 (PGE_2). AGE-2 and AGE-3 induced the expressions of adhesion molecule, the cytokine production, and the lymphocyte proliferation. PGE_2 concentration-dependently inhibited the actions of AGE-2 and AGE-3. The effects of PGE_2 were mimicked by an E-prostanoid $(EP)_2$-receptor agonist, 11,15-O-dimethyl prostaglandin E_2 (ONO-AE1-259-01), and an EP_4 receptor agonist, 16-(3-methoxymethyl)phenyl-ω-tetranor-3,7-dithia prostaglandin E_1 (ONO-AE1-329). An EP_2-receptor antagonist, 6-isopropoxy-9-oxaxanthene-2-carboxylic acid (AH6809), and an EP_4-receptor antagonist, (4*Z*)-7-[(rel-1*S*,2*S*,5*R*)-5-(1,1′-biphenyl-4-yl)methoxy)-2-(4-morpholinyl)-3-oxocyclopentyl]-4-heptenoic acid (AH23848), inhibited the actions of PGE_2. The stimulation of EP_2 and EP_4 receptors is reported to increase cAMP levels. The effects of PGE_2 were reversed by a protein kinase A (PKA) inhibitor, H89, and mimicked by a dibutyryl cAMP and an adenylate cyclase activator, forskolin. These results as a whole indicated that PGE_2 inhibited the actions of AGE-2 and AGE-3 via EP_2/EP_4 receptors and the cAMP/PKA pathway.

It is known that sugars, including glucose, fructose, and triose, react with amino groups of proteins nonenzymatically, leading to the formation of advanced glycation end product (AGE) (Brownlee et al., 1988). AGEs, a heterogeneous group of complex structures, form nonenzymatically when reducing sugars react with free amino groups on proteins, lipids, or nucleic acids. The formation and accumulation of AGEs occur at an accelerated rate in diabetic patients and may participate in the pathogenesis of diabetic micro- and macrovascular complications (Bierhaus et

This work was supported in part by the Japan Society for the Promotion of Science [Grants 18590509, 20590539, 17659159, 19659061, 21659141, 21390071, and 215905694]; the Scientific Research from Ministry of Health, Labor, and Welfare of Japan; and the Takeda Science Foundation.
Article, publication date, and citation information can be found at http://jpet.aspetjournals.org.
doi:10.1124/jpet.109.157594.

ABBREVIATIONS: AGE, advanced glycation end product; RAGE, receptor for advanced glycation end product; NF-κB, nuclear factor κB; TNF, tumor necrosis factor; IL, interleukin; ICAM, intercellular adhesion molecule; IFN, interferon; PBMC, peripheral blood mononuclear cell; PGE_2, prostaglandin E_2; COX, cyclooxygenase; AH6809, 6-isopropoxy-9-oxaxanthene-2-carboxylic acid; AH23848, [1α(*Z* BSA, bovine serum albumin; dbcAMP, dibutyryl cAMP; FITC, fluorescein isothiocyanate; mAb, monoclonal antibody; ELISA, enzyme-linked immunosorbent assay; sRAGE, soluble form of RAGE; PKA, protein kinase A; NS-398, *N*-[2-(cyclohexyloxyl)-4-nitrophenyl]-methane sulfonamide; EP, E-prostanoid; ONO-AE1-259-01, 11,15-O-dimethyl prostaglandin E_2; ONO-AE1-329, 16-(3-methoxymethyl)phenyl-ω-tetranor-3,7-dithia prostaglandin E_1; AH23848, (4*Z*)-7-[(rel-1S,2S,5R)-5-(1,1′-biphenyl-4-yl)methoxy)-2-(4-morpholinyl)-3-oxocyclopentyl]-4-heptenoic acid; ONO-DI-004, 17S-2,5-ethano-6-oxo-17,20-dimethyl prostaglandin E_1; ONO-AE-248, 16S-9-deoxy-9β-chloro-15-deoxy-16-hydroxy-17,17-trimethylene-19,20-didehydro prostaglandin F_2.

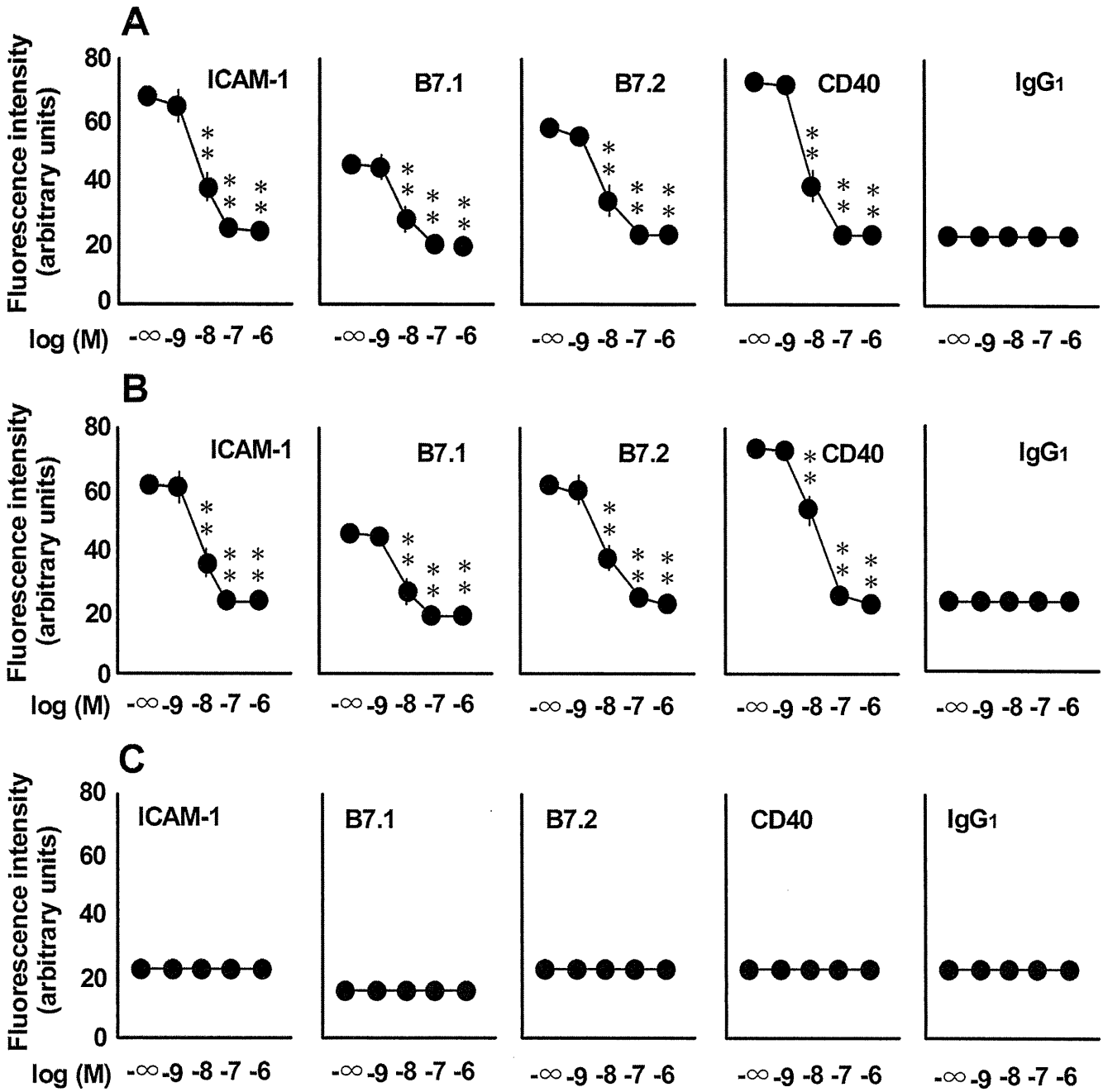

Fig. 1. The effects of PGE_2 on AGE-2- and AGE-3-induced expressions of ICAM-1, B7.1, B7.2, and CD40 on monocytes PBMC at 1×10^6 cells/ml were incubated with PGE_2 at increasing concentrations from 1 nM to 1 μM in the presence of AGE-2 (A), AGE-3 (B), and BSA (C) at 100 μg/ml for 24 h. The expressions of ICAM-1, B7.1, B7.2, and CD40 on monocytes were determined by flow cytometry. Isotype-matched control represents FITC-conjugated IgG1. The results are expressed as the means ± S.E.M. of five donors with triplicate determinations. **, $P < 0.01$ compared with the value for AGE-2 and AGE-3. When an error bar was within a symbol, the bar was omitted.

al., 1998; Fukami et al., 2004). It provided direct immunochemical evidence of the existence of four distinct AGE structures, including AGE-2, AGE-3, AGE-4, and AGE-5, within AGE-modified proteins and peptides (Takeuchi and Yamagishi, 2004). Among the various subtypes of AGE, it has been shown that glyceraldehyde-derived AGE (AGE-2) and glycolaldehyde-derived AGE (AGE-3) are the main AGE structures detectable in the serum of diabetic patients. Toxic AGE structures, AGE-2 and AGE-3, have diverse biological activities on vascular wall cells, mesangial cells, Schwann cells, malignant melanoma cells, and cortical neurons (Okamoto et al., 2002; Yamagishi et al., 2002). AGE-2 plays roles in the development of atherosclerosis (Takeuchi et al., 2000). The interaction between AGEs and the receptor for AGEs (RAGE) perturbs a variety of vascular homeostatic functions and thus may contribute to diabetic vasculopathy (Schmidt et al., 1994; Wautier et al., 1996; Park et al., 1998). AGEs and RAGE are reported to be detected in atherosclerotic plaque of diabetic patients (Cuccurullo et al., 2006). A recent study

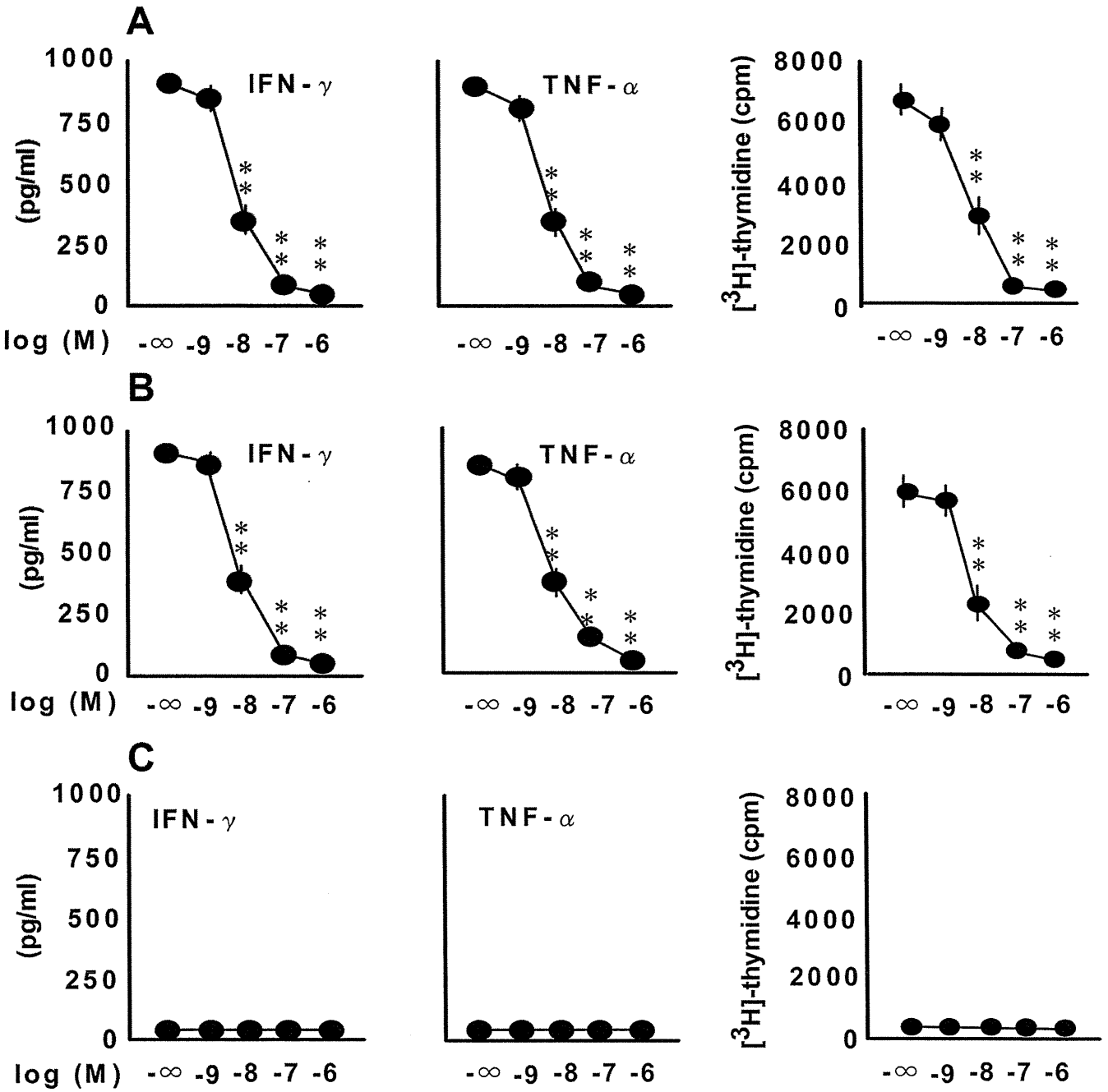

Fig. 2. The effects of PGE_2 on AGE-2- and AGE-3-induced production of IFN-γ and TNF-α and the lymphocyte proliferation in PBMC. The effect of PGE_2 at increasing concentrations from 1 nM to 1 μM in the presence of AGE-2 (A), AGE-3 (B), and BSA (C) at 100 μg/ml on IFN-γ and TNF-α concentrations in conditioned media was determined by ELISA. The lymphocyte proliferation was determined by [^{3}H]thymidine uptake as described under *Materials and Methods*. The results are expressed as the means ± S.E.M. of five donors with triplicate determinations. **, $P < 0.01$ compared with the value for AGE-2 and AGE-3. When an error bar was within a symbol, the bar was omitted.

reported that RAGE expression is associated with apoptotic smooth muscle cells and macrophages, suggesting that RAGE may promote plaque destabilization (Burke et al., 2004). It is reported that AGE-modified proteins can induce various proinflammatory and procoagulant cellular responses resulting from nuclear factor κB (NF-κB) activation (Yan et al., 1994), including the expression of vascular cell adhesion molecule-1, tumor necrosis factor (TNF)-α, interleukin (IL)-6, and tissue factor (Schmidt et al., 1994, 1995; Miyata et al., 1996; Bierhaus et al., 1997; Hofmann et al., 1999).

Microinflammation plays roles in the pathogenesis of diabetic vascular complications. It is reported that diabetes has more macrophage and T-cell infiltration in atherosclerotic plaques (Burke et al., 2004). Activation of monocytes/macrophages and T cells induces the progression of inflammatory atherosclerotic plaques (Stoll and Bendszus, 2006). The enhanced expression of adhesion molecule, including intercel-